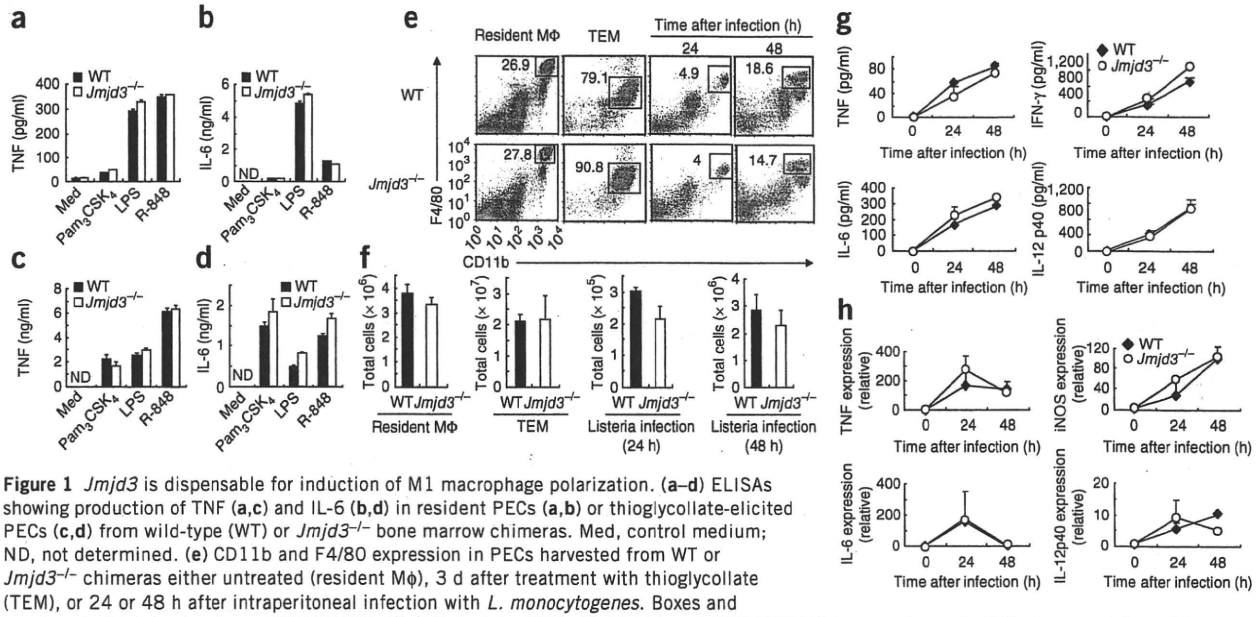

Figure 1 *Jmjd3* is dispensable for induction of M1 macrophage polarization. (**a–d**) ELISAs showing production of TNF (**a,c**) and IL-6 (**b,d**) in resident PECs (**a,b**) or thioglycollate-elicited PECs (**c,d**) from wild-type (WT) or *Jmjd3*$^{-/-}$ bone marrow chimeras. Med, control medium; ND, not determined. (**e**) CD11b and F4/80 expression in PECs harvested from WT or *Jmjd3*$^{-/-}$ chimeras either untreated (resident Mϕ), 3 d after treatment with thioglycollate (TEM), or 24 or 48 h after intraperitoneal infection with *L. monocytogenes*. Boxes and numbers indicate percentage of F4/80^{+}CD11b^{+} cells in total PECs. (**f**) Numbers of F4/80^{+}CD11b^{+} macrophages in PECs harvested from WT or *Jmjd3*$^{-/-}$ chimeras either untreated, 3 d after thioglycollate treatment or 24 or 48 h after intraperitoneal infection with *L. monocytogenes*. (**g**) ELISAs showing concentrations of TNF, IL-6, IFN-γ and IL-12p40 in the sera of WT or *Jmjd3*$^{-/-}$ chimeras infected with *L. monocytogenes*. (**h**) Quantitative PCR analysis showing expression of TNF, IL-6, IL-12p40 and iNOS mRNAs (relative to 18S rRNA) in PECs in mice infected with *L. monocytogenes*. Results are representative of four (**c–f**) or two (**a,b,g,h**) independent experiments (error bars indicate s.d.).

In addition to regulation by transcription factors, epigenetic regulation is essential for controlling proper gene expression[16]. Histone modifications, particularly at the N-terminal tails, and dynamic chromatin remodeling have been shown to be important for controlling sets of genes. In the case of histone modification, trimethylation of H3K4 is associated with active gene transcription, whereas trimethylation of H3K9, H3K27 and H4K20 is linked to silencing of gene expression[16,21,22]. The methylation of H3K27 is mediated by the Polycomb repressive complex-2 (PRC2), composed of Ezh2, Suz12 and Eed (ref. 23). Proteins harboring a Jumonji-C (JmjC) domain, such as Jmjd3, Utx and Uty, are known to act as H3K27 demethylases, catalyzing the conversion of H3K27me3 (trimethylated) to H3K27me1 (monomethylated)[24–26].

It has been reported that the expression of *Jmjd3* is induced in macrophages by TLR stimuli in an NF-κB–dependent fashion[26]. *Jmjd3* has also been identified as an early TLR-inducible gene in mouse macrophages by microarray analysis[27]. H3K27 trimethylation is implicated in the silencing of gene expression, and it has been shown that Jmjd3 is recruited to transcription start sites (TSSs) that have abundant RNA polymerase II and H3K4me3 (ref. 28). Jmjd3 is reported to fine-tune macrophage activation by controlling *Bmp2* and *Hox* expression[26]. Furthermore, Jmjd3 has been linked to the control of development through the regulation of *Hox*, and to oncogenesis through promotion of the expression of *Ink4a*[29,30]. Here we report the role of Jmjd3 *in vivo* in controlling M2 macrophage polarization and identify *Irf4* as a Jmjd3 target gene crucial for the regulation of macrophages.

RESULTS

Generation of *Jmjd3*$^{-/-}$ mice

To investigate the functional roles of Jmjd3 in immune responses *in vivo*, we generated *Jmjd3*$^{-/-}$ mice (**Supplementary Fig. 1a,b**). Reverse-transcription PCR analysis showed that the expression of *Jmjd3* was abrogated in *Jmjd3*$^{-/-}$ mouse embryonic fibroblasts (**Supplementary Fig. 1c**). *Jmjd3*$^{-/-}$ mice died perinatally, and adult *Jmjd3*$^{-/-}$ mice were not obtained (**Supplementary Fig. 2a**). Histological examination revealed that alveolar cell walls were thickened with tissues, and almost no air space was observed in lungs of *Jmjd3*$^{-/-}$ neonates (**Supplementary Fig. 2b**), suggesting that the postnatal lethal phenotype of *Jmjd3*$^{-/-}$ mice is due to premature development of lung tissues. To analyze the role of *Jmjd3* in hematopoietic cells, we obtained fetal liver cells from *Jmjd3*$^{-/-}$ E15.5 embryos and established bone marrow–chimeric mice. Flow cytometry revealed that populations of T cells, B cells, conventional dendritic cells, plasmacytoid dendritic cells, natural killer cells, neutrophils, F4/80^{+}CD11b^{+} macrophages and Ly6C^{hi}CD11b^{+} inflammatory monocytes in the spleen were similar between wild-type and *Jmjd3*$^{-/-}$ chimeras (**Supplementary Fig. 3**). Proliferative responses of splenic T and B cells to mitogens and antigen receptor stimuli were also not altered (**Supplementary Fig. 4**). Furthermore, *Jmjd3*$^{-/-}$ splenic T cells differentiated into either type 1 or type 2 helper T cells (T_H1 and T_H2) produced normal amounts of IFN-γ or IL-4, respectively (**Supplementary Fig. 5**). These results indicate that T cells lacking *Jmjd3* are capable of differentiating into T_H1 and T_H2 cells in response to cytokines.

Jmjd3 is dispensable for M1 macrophages

As *Jmjd3* is a TLR-inducible gene in macrophages, we first examined cytokine production of peritoneally resident and thioglycollate-elicited peritoneal exudate cells (PECs) in response to TLR ligands including lipopeptide (Pam_3CSK_4, a TLR2 ligand), lipopolysaccharide (LPS, a TLR4 ligand), imidazoquinoline analog (R-848, a TLR7 ligand) and oligonucleotide with a CpG motif (CpG-DNA, a TLR9 ligand). Production of TNF and IL-6 in response to TLR ligands did not differ between wild-type and *Jmjd3*$^{-/-}$ tissue-resident macrophages and thioglycollate-elicited PECs (**Fig. 1a–d**). PECs elicited

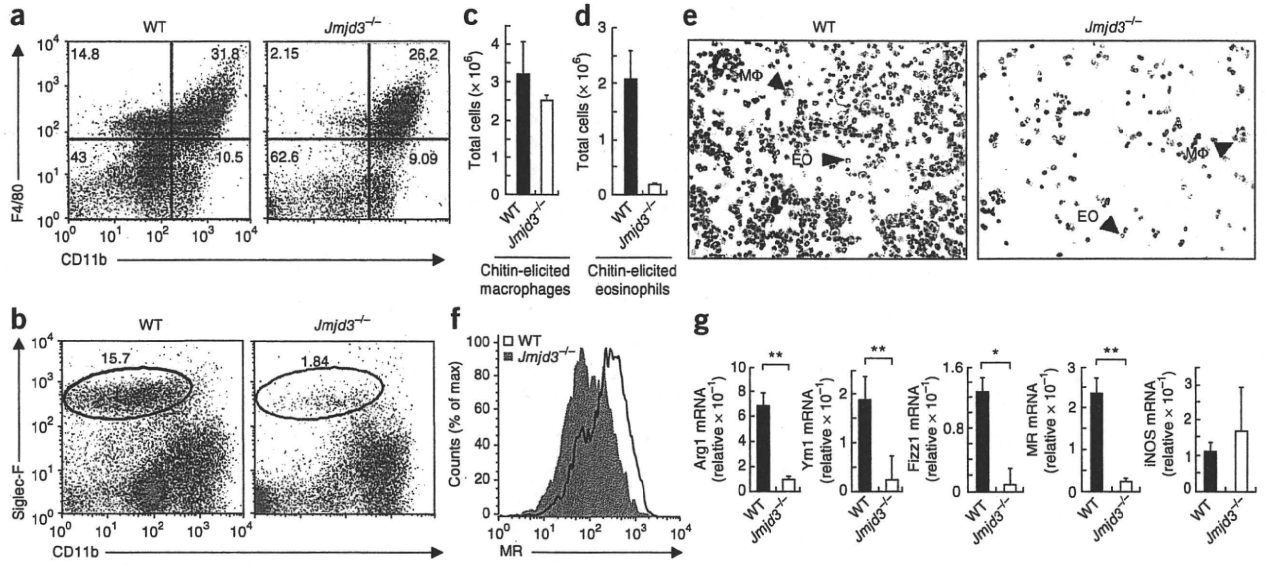

Figure 2 Crucial role of *Jmjd3* in M2 macrophage polarization in response to chitin administration. (**a**,**b**) Expression of CD11b and either F4/80 (**a**) or Siglec-F (**b**) in PECs harvested from wild-type (WT) or *Jmjd3*$^{-/-}$ chimeric mice 2 d after peritoneal injection with chitin. Quadrants and numbers in **a** indicate percentage of cells in each gate (F4/80$^+$CD11b$^+$, F4/80$^+$CD11b$^-$, F4/80$^-$CD11b$^+$ and F4/80$^-$CD11b$^-$); circles and numbers in **b** indicate percentage of Siglec-F$^+$ eosinophils in total PECs. (**c**,**d**) Numbers of F4/80$^+$CD11b$^+$ macrophages (**c**) or Siglec-F$^+$ eosinophils (**d**) in PECs harvested from WT or *Jmjd3*$^{-/-}$ chimeric mice 2 d after peritoneal injection with chitin. (**e**) Cell types within PEC population from chitin-treated mice, stained with Diff-Quick in cytospin centrifuges. Mϕ, macrophages; EO, eosinophils. (**f**) Surface MR expression on peritoneal F4/80$^+$CD11b$^+$ macrophages from chitin-treated mice. Graph shows MR expression on macrophages on horizontal axis. (**g**) Quantitative PCR showing expression of Arg1, Ym1, Fizz1, MR and iNOS mRNAs (relative to 18S rRNA). Total RNA was prepared from PECs 48 h after administration of chitin. $^*P < 0.05$; $^{**}P < 0.01$ (two-tailed Student's *t*-test). Results are representative of five (**a**–**d**), two (**e**) or three (**f**,**g**) independent experiments (error bars indicate s.d.).

by peptone treatment of wild-type or *Jmjd3*$^{-/-}$ chimeras also produced similar amounts of TNF and IL-6 in response to TLR ligand stimulation (**Supplementary Fig. 6a**). Flow cytometry revealed that the proportions of F4/80$^+$CD11b$^+$Gr1$^-$ cells among resident and thioglycollate-elicited PECs did not differ between wild-type and *Jmjd3*$^{-/-}$ chimeras (**Fig. 1e** and **Supplementary Fig. 7**). The total number of peritoneally resident macrophages, thioglycollate-elicited macrophages and peptone-elicited macrophages was not changed in *Jmjd3*$^{-/-}$ chimeras (**Fig. 1f** and **Supplementary Fig. 6b**). We then examined the role of Jmjd3 in M1 macrophage polarization in response to *Listeria monocytogenes* infection. When *L. monocytogenes* was inoculated intraperitoneally, production of proinflammatory cytokines in the sera was similar in wild-type and *Jmjd3*$^{-/-}$ chimeras (**Fig. 1g**). F4/80$^+$CD11b$^+$Gr1$^+$ macrophages, F4/80^{int}CD11b$^+$Gr1^{hi} neutrophils, and F4/80$^-$CD11b^{int}B220$^+$ and F4/80$^-$CD11b$^-$B220$^+$ B cells were examined in PECs prepared from *L. monocytogenes*–infected mice (**Supplementary Fig. 8**). The number of macrophages recruited to the peritoneal cavity was similar in wild-type and *Jmjd3*$^{-/-}$ chimeras (**Fig. 1e**,**f**). Furthermore, the expression of genes encoding TNF, IL-6, IL-12p40 and iNOS in PECs were similarly upregulated (**Fig. 1h**). Collectively, these data suggest that Jmjd3 is not involved in the generation and recruitment of M1 macrophages in response to inflammatory reagents and bacterial infection *in vivo*.

Jmjd3 is needed for M2 polarization to chitin

Chitin is a polymerized sugar and a structural component of helminths, arthropods and fungi[31]. It has been shown that chitin administration recruits macrophages with the M2 phenotype to the site of administration, which are important for subsequent recruitment of eosinophils[32,33]. Indeed, we found that intraperitoneal administration of chitin recruited F4/80$^+$CD11b$^+$ macrophages (**Fig. 2a**), Siglec-F$^+$CCR3$^+$CD4$^-$ eosinophils and CD11b^{int}B220$^+$ B cells to the peritoneal cavity after 48 h in wild-type mice (**Fig. 2b** and **Supplementary Fig. 9**). Whereas the number of chitin-elicited F4/80$^+$CD11b$^+$ macrophages was similar between wild-type and *Jmjd3*$^{-/-}$ chimeras (**Fig. 2c**), the recruitment of eosinophils was severely impaired in *Jmjd3*$^{-/-}$ chimeras (**Fig. 2b–e**). Furthermore, the expression of MR on chitin-elicited macrophages was severely impaired in *Jmjd3*$^{-/-}$ chimeras (**Fig. 2f**). Chitin-elicited macrophages, but not eosinophils or B cells, expressed high levels of mRNA encoding Arg1, Ym1, Fizz1 and MR, the hallmarks of M2 macrophages (**Supplementary Fig. 10**). The expression of genes encoding Arg1, Ym1, Fizz1 and MR was considerably lower in chitin-induced PECs obtained from *Jmjd3*$^{-/-}$ chimeras compared with wild-type controls, whereas expression of the gene encoding iNOS, associated with M1 macrophages, was not altered (**Fig. 2g**). Of note, the numbers of eosinophils circulating in the blood were similar in wild-type and *Jmjd3*$^{-/-}$ chimeric mice, suggesting that eosinophil development was not impaired by *Jmjd3* deficiency (data not shown). Together, these results suggest Jmjd3 is necessary for M2 macrophage polarization in response to chitin administration.

Role of *Jmjd3* in helminth infection

Next we investigated whether Jmjd3 contributes to the responses against helminth infection *in vivo*. We used the *Nippostrongylus brasiliensis* infection model, which induces a strong type 2 immune response in the lung. Bronchoalveolar lavage (BAL) staining 5 and 13 d after infection revealed that macrophages were similarly recruited to the lung in wild-type and *Jmjd3*$^{-/-}$ bone marrow chimeras (**Fig. 3a**,**b**).

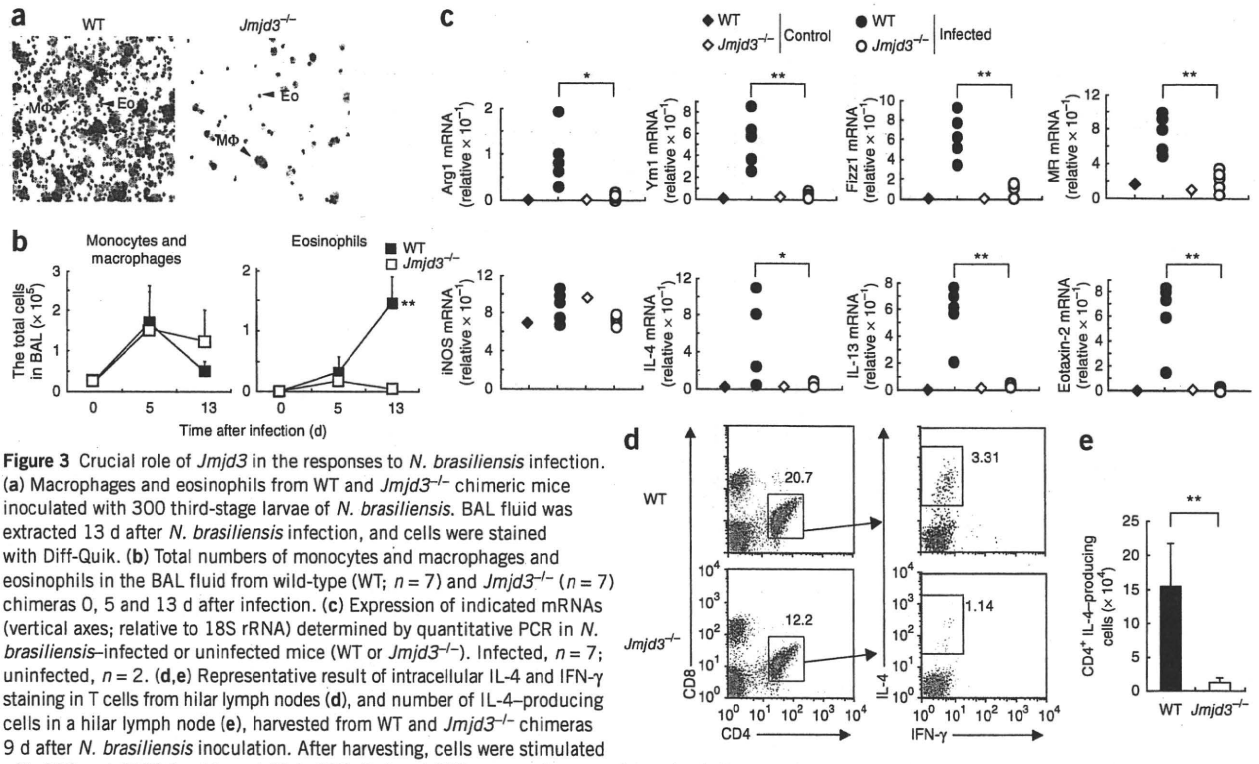

Figure 3 Crucial role of *Jmjd3* in the responses to *N. brasiliensis* infection. (**a**) Macrophages and eosinophils from WT and *Jmjd3*$^{-/-}$ chimeric mice inoculated with 300 third-stage larvae of *N. brasiliensis*. BAL fluid was extracted 13 d after *N. brasiliensis* infection, and cells were stained with Diff-Quik. (**b**) Total numbers of monocytes and macrophages and eosinophils in the BAL fluid from wild-type (WT; $n = 7$) and *Jmjd3*$^{-/-}$ ($n = 7$) chimeras 0, 5 and 13 d after infection. (**c**) Expression of indicated mRNAs (vertical axes; relative to 18S rRNA) determined by quantitative PCR in *N. brasiliensis*–infected or uninfected mice (WT or *Jmjd3*$^{-/-}$). Infected, $n = 7$; uninfected, $n = 2$. (**d**,**e**) Representative result of intracellular IL-4 and IFN-γ staining in T cells from hilar lymph nodes (**d**), and number of IL-4–producing cells in a hilar lymph node (**e**), harvested from WT and *Jmjd3*$^{-/-}$ chimeras 9 d after *N. brasiliensis* inoculation. After harvesting, cells were stimulated with CD3 and CD28 for 4 h, and CD4, CD8, IL-4 and IFN-γ expression were determined. Boxes and numbers indicate percentages of CD4$^+$ cells in hilar lymph node cells and IL-4–producing cells in CD4$^+$ cells. $^*P < 0.05$; $^{**}P < 0.01$ (two-tailed Student's *t*-test). Results are representative of two experiments with four mice per group (**a**,**b**), a single experiment with seven mice per group (**c**) or a single experiment with five mice (**d**,**e**) (error bars indicate s.d.).

However, the recruitment of eosinophils was severely impaired in *Jmjd3*$^{-/-}$ chimeric mice (**Fig. 3b**). To investigate the characteristics of recruited macrophages, we extracted RNA from lung tissue 5 d after *N. brasiliensis* infection. M2 markers such as Arg1, Ym1, Fizz1 and MR were barely expressed in *Jmjd3*$^{-/-}$ chimeras (**Fig. 3c**). Furthermore, induction of genes encoding the eosinophil-recruiting chemokine eotaxin-2 and the T_H2-inducing cytokines IL-4 and IL-13 was severely impaired in *Jmjd3*$^{-/-}$ chimeric mice (**Fig. 3c**). Thus, we

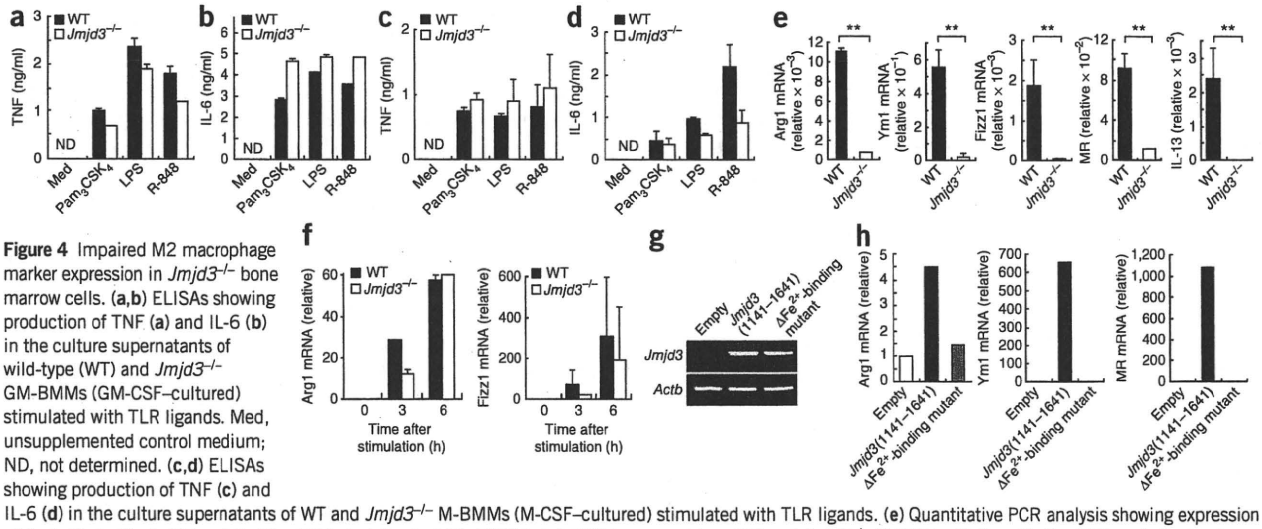

Figure 4 Impaired M2 macrophage marker expression in *Jmjd3*$^{-/-}$ bone marrow cells. (**a**,**b**) ELISAs showing production of TNF (**a**) and IL-6 (**b**) in the culture supernatants of wild-type (WT) and *Jmjd3*$^{-/-}$ GM-BMMs (GM-CSF–cultured) stimulated with TLR ligands. Med, unsupplemented control medium; ND, not determined. (**c**,**d**) ELISAs showing production of TNF (**c**) and IL-6 (**d**) in the culture supernatants of WT and *Jmjd3*$^{-/-}$ M-BMMs (M-CSF–cultured) stimulated with TLR ligands. (**e**) Quantitative PCR analysis showing expression of Arg1, Ym1, Fizz1, MR and IL-13 mRNAs (relative to 18S rRNA) in total RNA prepared from WT and *Jmjd3*$^{-/-}$ M-BMMs. (**f**) Quantitative PCR analysis showing expression of Arg1 and Fizz1 mRNAs (relative to 18S rRNA) in total RNA prepared from WT and *Jmjd3*$^{-/-}$ M-BMMs stimulated with IL-4 (10 ng/ml). (**g**,**h**) Reverse-transcription PCR showing expression of *Jmjd3* cDNA, with *Actb* cDNA as an expression control (**g**), and quantitative PCR showing expression of Arg1, Ym1 and MR mRNAs (relative to empty-vector control; **h**), in total RNA of *Jmjd3*$^{-/-}$ M-BMMs generated from bone marrow cells infected with retroviruses expressing WT Jmjd3 (amino acid residues 1141–1641) or its iron binding–deficient mutant. Results are representative of four (**a**–**d**), three (**e**,**f**) or two (**g**,**h**) independent experiments (error bars indicate s.d.).

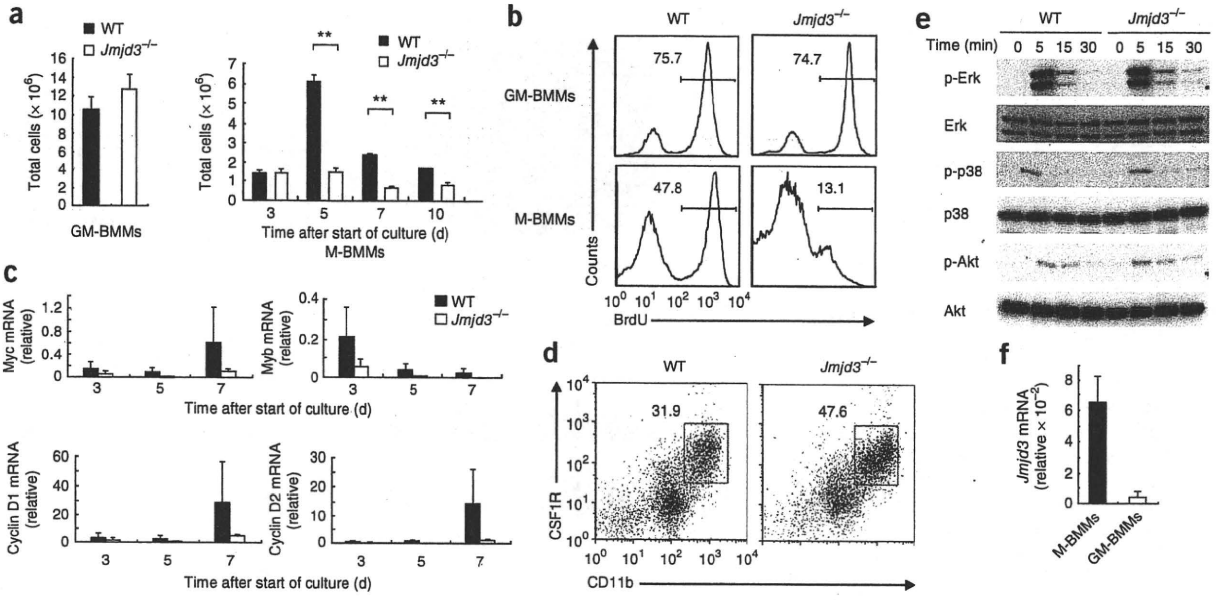

Figure 5 *Jmjd3* is required for the cell-cycle progression of M-BMMs. (**a**) Numbers of GM-BMMs and M-BMMs generated from wild-type (WT) and *Jmjd3*$^{-/-}$ bone marrow cells. Bone marrow cells from WT and *Jmjd3*$^{-/-}$ chimeras were cultured in the presence of GM-CSF for 5 d or M-CSF for time indicated (horizontal axis), and the number of adherent CD11b^{+} cells was counted. (**b**) Incorporation of BrdU in WT and *Jmjd3*$^{-/-}$ GM-BMMs and M-BMMs incubated in the presence of BrdU for 24 h. Incorporation was examined by intracellular staining with anti-BrdU. (**c**) Quantitative PCR showing expression of mRNAs encoding c-Myc, c-Myb, cyclin D1 and cyclin D2 (relative to 18S rRNA) in WT and *Jmjd3*$^{-/-}$ M-BMMs. (**d**) Surface expression of colony stimulating receptor (CSF1R) and CD11b on WT and *Jmjd3*$^{-/-}$ M-BMMs. Boxes and numbers indicate percentages of CSF1R-expressing M-BMMs. (**e**) Expression of phosphorylated (p-) and unphosphorylated Erk, p38 and Akt in WT and *Jmjd3*$^{-/-}$ M-BMMs stimulated with M-CSF (50 ng/ml). Cells were starved for 4 h before stimulation, and cell lysates were subjected to immunoblot analysis with antibodies to p-Erk, p-p38 and p-Akt. The membrane was stripped and reprobed for expression of Erk, p38 and Akt. (**f**) Quantitative PCR showing Jmjd3 mRNA expression (relative to 18S rRNA) by M-BMMs and GM-BMMs. $*P < 0.05$; $**P < 0.01$ (two-tailed Student's *t*-test). Results are representative of four (**a**), three (**b**,**f**) or two (**c**–**e**) independent experiments (error bars indicate s.d.).

investigated the activation of T cells in the pulmonary lymph nodes 9 d after *N. brasiliensis* infection. Whereas CD4^{+} T cells prepared from wild-type pulmonary lymph nodes expressed IL-4, but not IFN-γ, the frequency of IL-4–producing CD4^{+} T cells was severely impaired in pulmonary T cells prepared from *Jmjd3*$^{-/-}$ chimeric mice, suggesting that Jmjd3-mediated M2 macrophage activation is crucial for *N. brasiliensis* to induce T_H2 responses in the lung (**Fig. 3d,e**). However, histological changes in the intestine were not severely impaired in *Jmjd3*$^{-/-}$ chimeric mice (data not shown). Collectively, our results demonstrate that Jmjd3 is essential for mounting immune responses to helminth infection, directing M2 macrophage polarization in the lung but not in the small intestine.

Role of *Jmjd3* in M2 macrophage generation in response to M-CSF

Numerous studies have shown that GM-CSF induces M1 macrophages from bone marrow cells and M-CSF induces M2 macrophages from bone marrow cells[12–15]. When we used GM-CSF to generate macrophages, similar amounts of TNF and IL-6 were produced in wild-type and *Jmjd3*$^{-/-}$ chimeras in response to TLR ligands from adherent CD11b^{+} macrophages (termed GM-BMMs, for GM-CSF–induced bone marrow–derived macrophages; **Fig. 4a,b**). In contrast, production of IL-6, but not TNF, in response to TLR ligand stimulation was partially impaired in *Jmjd3*$^{-/-}$ bone marrow cultured in the presence of M-CSF (M-BMMs; **Fig. 4c,d**). Furthermore, the expression of genes encoding Arg1, Ym1, Fizz1, MR and IL-13 was severely impaired in M-BMMs from *Jmjd3*$^{-/-}$ chimeras (**Fig. 4e**), which indicates that *Jmjd3* is crucial for expression of hallmark M2 genes in M-BMMs. Jmjd3 is involved in the response of macrophages to IL-4 stimulation[34]; nevertheless, Arg1 and Fizz1 gene expression were similar after IL-4 stimulation in wild-type and *Jmjd3*$^{-/-}$ M-BMMs (**Fig. 4f**), suggesting that the responses to IL-4 were not impaired in *Jmjd3*$^{-/-}$ M-BMMs. We then used microarray analysis to examine the gene expression profiles in wild-type and *Jmjd3*$^{-/-}$ M-BMMs with or without LPS stimulation. The expression of 1,371 genes was more than 50% lower in unstimulated *Jmjd3*$^{-/-}$ M-BMMs compared with wild-type (**Supplementary Table 1**). In addition to *Arg1*, *Chi3l3* and *Fizz1*, the expression of cytokine genes such as *Il2*, *Il3*, *Il4*, *Il5* and *Il13*, as well as that of chemokine genes such as *Ccl1*, *Ccl17*, *Ccl22* and *Ccl24*, was severely impaired in *Jmjd3*$^{-/-}$ M-BMMs (**Supplementary Table 1**). The expression of 2,188 genes was more than twofold higher in wild-type M-BMMs in response to LPS stimulation, and that of 436 genes was reduced by over 50% in LPS-stimulated *Jmjd3*$^{-/-}$ M-BMMs (**Supplementary Table 2**). For example, the expression of *Il6* and *Il12b* was partially impaired in *Jmjd3*$^{-/-}$ M-BMMs, consistent with a previous report (**Supplementary Table 2**). Therefore, Jmjd3 is important for inducing expression of a large set of genes, and some of these are related to M2 macrophage polarization in M-BMMs.

In addition to its JmjC domain, Jmjd3 contains a putative tetratricopeptide repeat domain in the N terminus. We therefore examined whether the demethylase activity of Jmjd3 is needed for the defect in M2 macrophage marker expression. We retrovirally expressed the C-terminal part of Jmjd3, containing the JmjC domain (amino acid residues 1141–1641), or its iron binding–deficient mutant (A1388H) in *Jmjd3*$^{-/-}$ bone marrow cells and then induced M-BMMs (**Fig. 4g**).

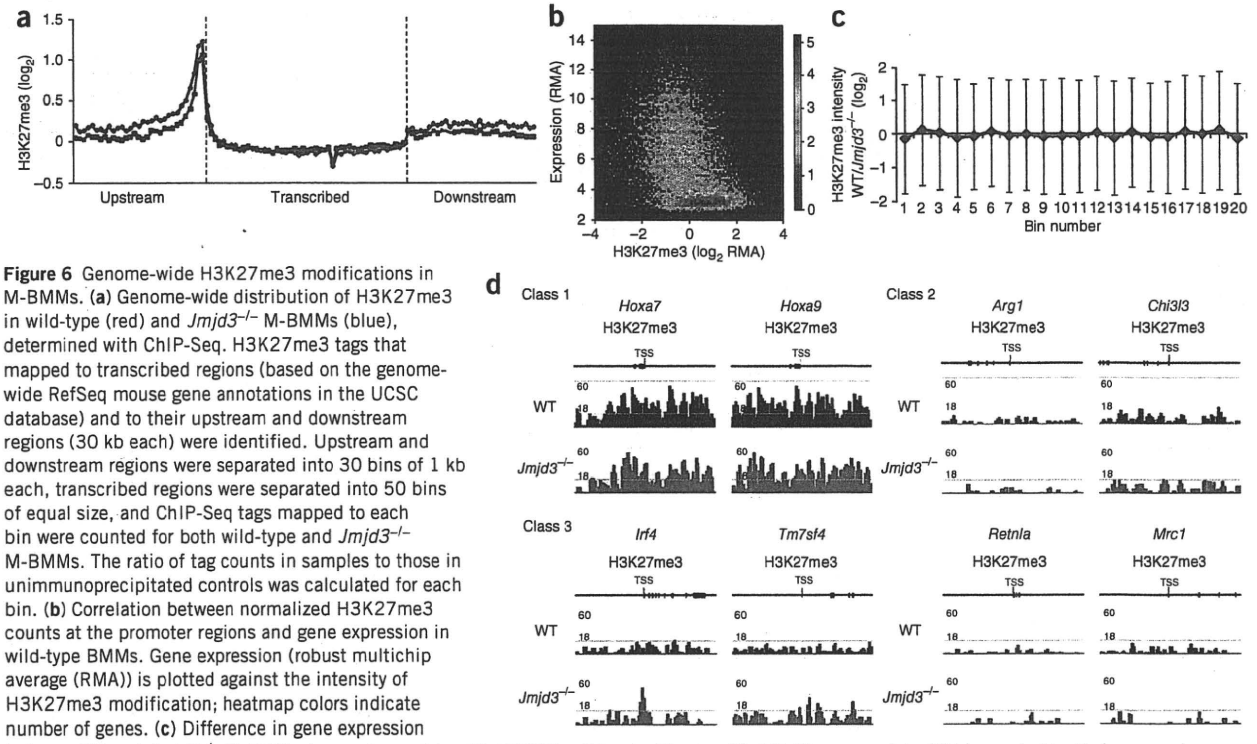

Figure 6 Genome-wide H3K27me3 modifications in M-BMMs. (**a**) Genome-wide distribution of H3K27me3 in wild-type (red) and *Jmjd3*$^{-/-}$ M-BMMs (blue), determined with ChIP-Seq. H3K27me3 tags that mapped to transcribed regions (based on the genome-wide RefSeq mouse gene annotations in the UCSC database) and to their upstream and downstream regions (30 kb each) were identified. Upstream and downstream regions were separated into 30 bins of 1 kb each, transcribed regions were separated into 50 bins of equal size, and ChIP-Seq tags mapped to each bin were counted for both wild-type and *Jmjd3*$^{-/-}$ M-BMMs. The ratio of tag counts in samples to those in unimmunoprecipitated controls was calculated for each bin. (**b**) Correlation between normalized H3K27me3 counts at the promoter regions and gene expression in wild-type BMMs. Gene expression (robust multichip average (RMA)) is plotted against the intensity of H3K27me3 modification; heatmap colors indicate number of genes. (**c**) Difference in gene expression between WT and *Jmjd3*$^{-/-}$ M-BMMs does not correlate with H3K27me3 levels. We classified RefSeq genes into 20 bins sorted by their expression difference between WT and *Jmjd3*$^{-/-}$ cells. Bins are numbered from low to high WT/*Jmjd3*$^{-/-}$ expression ratio. The average H3K27 modification intensity was calculated in each bin. (**d**) H3K27me3 modifications of wild-type (WT, blue) and *Jmjd3*$^{-/-}$ (red) cells on class 1 genes (*Hoxa7* and *Hoxa9*), class 2 genes (*Arg1*, *Chi3l3* for Ym1, *Fizz1*, *Mrc1* for MR) and class 3 genes (*Irf4* and *Tm7sf4*). Gray lines indicate the threshold tag counts for WT (18 tags) and *Jmjd3*$^{-/-}$ M-BMMs (18 tags) corresponding to a false discovery rate of 1×10^{-6}.

The A1388H mutation has been shown to abrogate the H3K27 demethylase activity of Jmjd3 (ref. 26). Expression of the C-terminal part of Jmjd3 was sufficient to upregulate M2 marker genes such as *Arg1*, *Chi3l3* and *Mrc1* (**Fig. 4h**). In contrast, the expression of *Jmjd3* (A1388H) did not increase the expression of M2 marker genes, which indicates that the H3K27me3 demethylase activity of Jmjd3 is necessary and sufficient for expression of M2 marker genes in M-BMMs.

M-BMMs require *Jmjd3* for cell cycle progression

In addition to the impaired M2 marker expression, the total number of M-BMM cells in *Jmjd3*$^{-/-}$ chimeras was considerably lower than in the wild type at days 5 and 7 of culture with M-CSF (**Fig. 5a**), although the number of GM-BMM cells (M1) was not altered. We found 5-bromodeoxyuridine (BrdU) incorporation, a measure of cell division, was severely impaired in *Jmjd3*$^{-/-}$ M-BMMs compared with wild-type cells (**Fig. 5b**), whereas wild-type and *Jmjd3*$^{-/-}$ GM-BMMs incorporated BrdU similarly. These results indicate that Jmjd3 controls cell-cycle progression in response to M-CSF stimulation. Expression of cell cycle–regulatory proteins (c-Myc, c-Myb, cyclin D1 and cyclin D2) was impaired in *Jmjd3*$^{-/-}$ M-BMMs at day 5 of culture (**Fig. 5c**); however, the surface expression of M-CSF receptor (CSF-1R) was normal in *Jmjd3*$^{-/-}$ M-BMMs (**Fig. 5d**). Furthermore, *Jmjd3* deficiency did not affect activation of the intracellular signaling molecules Erk, p38 and Akt, as indicated by their phosphorylation in M-BMMs (**Fig. 5e**), implying that the cell proliferation defects in *Jmjd3*$^{-/-}$ M-BMMs are not due to less activation of MAP kinases or Akt. The expression of *Jmjd3* in M-BMMs was much higher than that in GM-BMMs (**Fig. 5f**), suggesting that differential expression of *Jmjd3* in M-BMMs and GM-BMMs determines the contribution of Jmjd3 to their proliferation. Together, these data indicate that Jmjd3 performs a key step in the generation of M-BMMs, but not GM-BMMs, by controlling cell proliferation downstream of CSF-1R signaling.

Genome-wide analysis of H3K27me3 controlled by Jmjd3

Next we analyzed the genome-wide distribution of H3K27 trimethylation in wild-type and *Jmjd3*$^{-/-}$ M-BMMs by chromatin immunoprecipitation–sequencing (ChIP-Seq) analysis. We obtained an overall picture of the H3K27me3 distribution in transcribed regions (based on the genome-wide RefSeq mouse gene annotations in the University of California, Santa Cruz database) and in regions 30 kb upstream and 30 kb downstream. High levels of H3K27me3 tags were detected surrounding TSSs in M-BMMs from wild-type and *Jmjd3*$^{-/-}$ chimeras (**Fig. 6a**). In contrast, H3K27me3 levels were low in transcribed loci compared with upstream and downstream regions (**Fig. 6a**). Notably, H3K27me3 signals at the promoter and downstream regions were higher in *Jmjd3*$^{-/-}$ M-BMMs compared with wild-type cells.

We then compared the gene expression data obtained by microarray experiments with H3K27 methylation status. Overall, H3K27me3 levels in regions close to the TSS (−5 to +1 kb) correlated negatively with gene expression in M-BMMs (correlation coefficient −0.441; **Fig. 6b**). Next, we sorted genes by their ratio of expression in wild-type and *Jmjd3*$^{-/-}$ M-BMMs and examined H3K27me3 levels. However, we did not detect a correlation between H3K27me3 status and the difference in gene expression in wild-type compared with *Jmjd3*$^{-/-}$ M-BMMs (**Fig. 6c**). These data suggest that only small numbers of genes were affected by the absence of *Jmjd3*, and most loci are regulated by Utx or by both Jmjd3 and Utx.

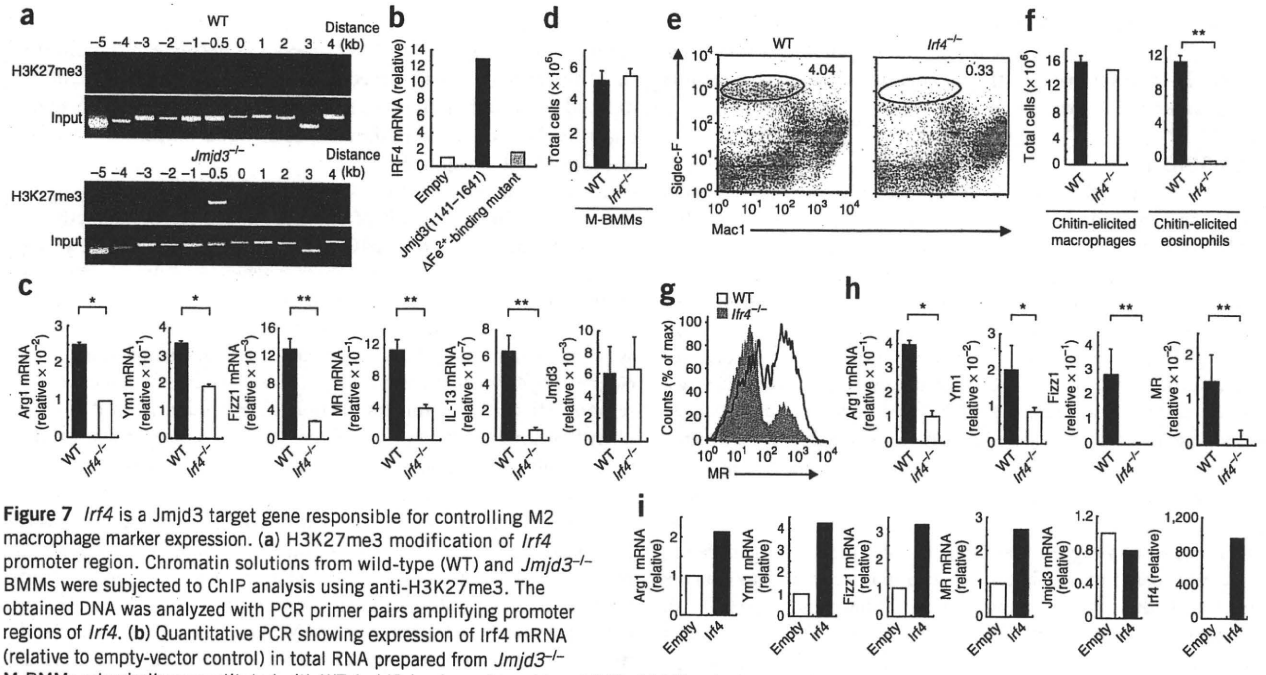

Figure 7 *Irf4* is a Jmjd3 target gene responsible for controlling M2 macrophage marker expression. (**a**) H3K27me3 modification of *Irf4* promoter region. Chromatin solutions from wild-type (WT) and *Jmjd3*$^{-/-}$ BMMs were subjected to ChIP analysis using anti-H3K27me3. The obtained DNA was analyzed with PCR primer pairs amplifying promoter regions of *Irf4*. (**b**) Quantitative PCR showing expression of Irf4 mRNA (relative to empty-vector control) in total RNA prepared from *Jmjd3*$^{-/-}$ M-BMMs retrovirally reconstituted with WT Jmjd3 (amino acid residues 1141–1641) or its iron binding–deficient mutant. (**c**) Quantitative PCR showing expression of M2 markers and Jmjd3 in bone marrow cells from WT and *Irf4*$^{-/-}$ mice cultured in the presence of M-CSF for 5 d. (**d**) Numbers of M-BMMs obtained from wild-type and *Irf4*$^{-/-}$ mice. (**e–g**) Macrophage and eosinophil recruitment (**e**), numbers of macrophages and eosinophils (**f**) and expression of MR (**g**) in macrophages from chitin-elicited PECs. WT and *Irf4*$^{-/-}$ mice were intraperitoneally treated with chitin, and PECs were prepared 48 h after treatment. Graph in **g** shows percentage of macrophages with the MR expression levels indicated on horizontal axis. (**h**) Quantitative PCR showing expression of M2 markers (relative to 18S rRNA) in total RNA prepared from PECs obtained from chitin-treated WT and *Irf4*$^{-/-}$ mice. (**i**) Quantitative PCR showing expression of M2 markers and Jmjd3 (relative to empty-vector control) in *Jmjd3*$^{-/-}$ M-BMMs in which Irf4 was ectopically expressed using retrovirus. $^{*}P < 0.05$; $^{**}P < 0.01$ (two-tailed Student's *t*-test). Results are representative of two (**a**,**b**,**i**) or three (**c–h**) independent experiments (error bars indicate s.d.).

Given the higher concentration of H3K27me3 tags in the region near the TSS, and the lack of overall correlation between expression changes and tag numbers, we focused on the promoter regions of individual genes that showed H3K27me3 peaks. We looked for peaks in wild-type and *Jmjd3*$^{-/-}$ M-BMM samples and divided the genome-wide set of genes into three different classes depending on H3K27me3 status (**Fig. 6d**). Class 1 genes harbored an H3K27me3 peak in wild-type M-BMMs. Class 2 genes did not have an H3K27me3 peak in either wild-type or *Jmjd3*$^{-/-}$ M-BMMs. Class 3 genes such as *Irf4* and *Tm7sf4* had an H3K27me3 peak in *Jmjd3*$^{-/-}$ but not in wild-type M-BMMs. We generated a table of 500 genes differentially expressed in wild-type and *Jmjd3*$^{-/-}$ M-BMMs, comparing H3K27 methylation status and gene expression from the microarray data (**Supplementary Table 3**).

Although *Hox* genes, such as *Hoxa7*, *Hoxa9* and *Tlx1* (also called *Hox11*), and *Bmp2* have been reported to be regulated by Jmjd3 (ref. 26), the H3K27 of their loci were highly trimethylated in M-BMMs both in the presence and absence of *Jmjd3*, and they therefore were assigned to class 1 (**Fig. 6d** and **Supplementary Table 3**). Furthermore, *Hox* and *Bmp2* gene expression was not lower in *Jmjd3*$^{-/-}$ M-BMMs (**Supplementary Table 3**), which indicates that these genes are not crucially regulated by Jmjd3 in M-BMMs. Furthermore, M2 marker genes, such as *Arg1*, *Chi3l3*, *Rentla* and *Mrc1*, were all in class 2, which indicates that their expression is not directly regulated by Jmjd3 (**Fig. 6d** and **Supplementary Table 3**). Thus, we proposed that transcription factors directly regulated by Jmjd3-mediated demethylation are responsible for the polarization of macrophages. When we searched genes categorized in class 3, we found *Irf4* and *Cebpb*. In particular, the promoter region close to the TSS of *Irf4* had a high H3K27me3 signal in *Jmjd3*$^{-/-}$ but not in wild-type M-BMMs (**Fig. 6d**).

Identification of *Irf4* as a Jmjd3 target gene

We confirmed by ChIP analysis that H3K27 at the promoter region of *Irf4* is differentially methylated in wild-type and *Jmjd3*$^{-/-}$ macrophages (**Fig. 7a**). Furthermore, when we retrovirally expressed the C-terminal region of Jmjd3 or its mutant in *Jmjd3*$^{-/-}$ macrophages, we found the expression of *Irf4* was demethylase activity dependent (**Fig. 7b**). These results demonstrate that *Irf4* is one of the Jmjd3 target genes in M-BMMs. Therefore, we examined the contribution of Irf4 to expression of mRNAs encoding Arg1, Ym1, Fizz1 and MR by using *Irf4*$^{-/-}$ mice. Induction of M2-related genes was severely impaired in *Irf4*$^{-/-}$ M-BMMs; in contrast, the expression of *Jmjd3* was similar between wild-type and *Irf4*$^{-/-}$ M-BMMs (**Fig. 7c**). Notably, the number of M-BMM cells was not lower in *Irf4*$^{-/-}$ mice (**Fig. 7d**). When chitin was administered peritoneally, recruitment of eosinophils, but not macrophages, was severely impaired in *Irf4*$^{-/-}$ mice (**Fig. 7e,f**). MR expression in chitin-elicited peritoneal macrophages was greatly impaired in *Irf4*$^{-/-}$ mice (**Fig. 7g**). In addition, the mRNA expression of the M2 macrophage markers encoding Arg1, Ym1, Fizz1 and MR was severely impaired in chitin-induced macrophages from *Irf4*$^{-/-}$ mice (**Fig. 7h**). These results demonstrate that Irf4 is crucial for the polarization of macrophages to M2 in M-BMMs and *in vivo* in response to chitin administration.

We then retrovirally expressed Irf4 in *Jmjd3*$^{-/-}$ M-BMMs and examined the expression of M2 marker genes (**Fig. 7i**). The expression

of Irf4 upregulated mRNAs encoding Arg1, Ym1, Fizz1 and MR in *Jmjd3*$^{-/-}$ M-BMMs, though the expression of Jmjd3 was unaltered (**Fig. 7i**). These results suggest that Irf4 contributes to the expression of M2 marker genes downstream of Jmjd3.

DISCUSSION

Here we focused on the role of Jmjd3 in macrophages mounting antibacterial and anti-parasitic responses. Whereas Jmjd3 was dispensable for M1 macrophage polarization, mice lacking *Jmjd3* did not mount proper M2 responses against helminth infection or chitin administration. Furthermore, bone marrow macrophages induced by M-CSF showed demethylase activity–dependent defects in expressing various genes, including M2 macrophage markers. Nevertheless, only a subset of genes had H3K27me3 levels differentially regulated by the presence or absence of *Jmjd3*. Among these genes, we found *Irf4* to be one of the direct targets of Jmjd3-mediated demethylation. Finally, we found that Irf4 is a transcription factor crucial for the induction of M2 macrophage responses.

Although *Jmjd3* is a TLR-inducible gene, *Jmjd3*$^{-/-}$ mice showed vigorous M1 macrophage activation in response to *Listeria* inoculation. These results suggest that *Jmjd3* is not essential for generating and recruiting M1 macrophages to bacterial infections. Our data are consistent with a previous report showing that gene expression in response to LPS stimulation is only modestly changed in macrophages lacking *Jmjd3* and that Jmjd3 in this case fine-tunes the transcriptional output[28]. TLR signaling upregulates genes involved not only in the promotion of inflammation, but also in termination or tissue remodeling. For instance, ATF3 and Zc3h12a are rapidly induced in response to TLR stimulation and inhibit inflammatory cytokine production[19,27]. It has been shown that M2 macrophages promote tissue remodeling as well as T_H2 responses. Thus, it is possible that *Jmjd3* induction functions as part of a feedback mechanism acting to repair inflammatory damage caused by TLR stimulation.

Chitin is an abundant structural component of helminths, crustaceans and fungi, and administration of chitin strongly induces M2 macrophage activation. Intraperitoneal administration of chitin recruited M2 macrophages and eosinophils in a Jmjd3- and Irf4-dependent fashion. These results indicate that the Jmjd3-*Irf4* axis is essential for M2 macrophage polarization to helminth infection.

However, addition of chitin to the macrophage culture did not stimulate the cells to upregulate M2 marker gene expression in our experiments (data not shown). Although TLR2 has been reported to mediate acute inflammation in response to chitin, another study has shown that chitin-mediated M2 macrophage activation is independent of MyD88, an adaptor molecule used by all TLRs (refs. 32,35). Currently, the mechanism by which chitin activates macrophages is not well understood. Moreover, it is still not clear what unique role Jmjd3 carries out in the generation of M2 macrophages in response to chitin and helminth infection. The identification of the chitin receptor(s) in the future will be vital for clarifying mechanisms of innate immune activation in response to helminth infection.

Jmjd3$^{-/-}$ mice also showed severe defects in recruiting M2 macrophages in response to *N. brasiliensis* infection. Although it is unknown which components of *N. brasiliensis* activate innate immune cells, Jmjd3-mediated H3K27me3 demethylation seems to be essential for macrophage responses to this parasite. Further studies are needed to identify the role of Jmjd3 in controlling infection with other helminths pathogenic to humans. M2 macrophages are known to be important for tumor cell survival and tissue remodeling in response to inflammation, in addition to the response against helminth infection[36]. Thus, it would be interesting to use this mouse model to explore how epigenetic regulation in macrophages promotes cancer progression or wound healing.

A previous report has found that *Jmjd3* expression is upregulated in response to IL-4 and that H3K27me3 levels decrease in response to IL-4 stimulation[34]. We observed that although M-BMMs and chitin-induced peritoneal macrophages showed severe defects in M2 macrophage marker expression in the absence of *Jmjd3*, *Jmjd3*$^{-/-}$ M-BMMs were capable of upregulating expression of genes representative of M2 macrophages in response to IL-4 stimulation. These findings suggest that IL-4 acts independently of Jmjd3-mediated H3K27 demethylation to promote M2 polarization. The same report[34] showed that H3K27me3 levels of various M2 marker genes were directly controlled by Jmjd3 to activate transcription. In contrast, our ChIP-Seq data demonstrate that H3K27me3 levels of most M2 marker genes, such as *Arg1*, are not changed in the absence of *Jmjd3*. Furthermore, deficiency in *Irf4*, one of the Jmjd3 target genes, resulted in defective M2 responses to chitin administration or M-CSF culture. Thus, it is more likely that Jmjd3 secondarily regulates M2 macrophage polarization by controlling expression of a set of transcription factors.

In addition to M2 marker gene expression, M-BMMs lacking *Jmjd3* showed proliferation defects in response to M-CSF stimulation. This is not due to impaired M-CSF receptor expression or defective activation of initial signaling molecules. Although the expression of genes involved in cell-cycle progression, such as those encoding c-Myc, cyclin D1 and cyclin D2, was impaired in *Jmjd3*$^{-/-}$ M-BMMs, H3K27me3 levels of these genes did not differ between wild-type and *Jmjd3*$^{-/-}$ M-BMMs. Furthermore, *Irf4*$^{-/-}$ M-BMMs did not show a defect in cell cycling (data not shown). Thus, it is possible that other Jmjd3 target genes are responsible for controlling the proliferation of M-BMMs.

ChIP-Seq analysis revealed that, in general, differences between wild-type and *Jmjd3*$^{-/-}$ M-BMM H3K27me3 levels at gene promoter regions were subtle. Nevertheless, gene expression profiles examined by microarray analysis were substantially different in wild-type and *Jmjd3*$^{-/-}$ M-BMMs, and the responses to chitin or helminth infection *in vivo* were severely impaired in *Jmjd3*$^{-/-}$ mice. Although it has been shown that *Hoxa* and *Bmp2* genes are potential targets of Jmjd3 (ref. 26), the expression of these genes was not lower in *Jmjd3*$^{-/-}$ cells, and the H3K27me3 levels were similar between wild-type and *Jmjd3*$^{-/-}$ M-BMMs. These results suggest that other H3K27 demethylases such as Utx and Uty compensate for the lack of *Jmjd3* in macrophages.

However, we identified Irf4 as one direct Jmjd3-specific target transcription factor. Irf4 has been shown to be involved in T_H2 cell polarization as well as in plasma cell differentiation and class-switch recombination in B cells[37,38]. It has also been reported that Irf4 functions in regulatory T cells to regulate T_H2 responses[39]. Indeed, *Irf4*$^{-/-}$ mice have been found to show defective T_H2 responses to *N. brasiliensis* infection[40]. Given that *Irf4*$^{-/-}$ mice did not induce M2 macrophages in response to chitin administration in our experiments, it is likely that the defects of macrophages in *Irf4*$^{-/-}$ mice also contribute to their abnormal responses to *N. brasiliensis* infection. In macrophages, Irf4 functions as a negative regulator of TLR signaling by associating with MyD88 (refs. 41,42).

Jmjd3$^{-/-}$ mice showed neonatal death due to a developmental defect in lung tissue. Although Jmjd3 directly regulated the expression of *Irf4* in macrophages, *Irf4*$^{-/-}$ mice did not show a developmental defect. Thus, Jmjd3 controls genes other than *Irf4* in the lung tissues for proper tissue development, and we focused solely on the role of this molecule in macrophages.

It is tempting to speculate that the change in epigenetic status is crucial for determining macrophage polarization. Future development of procedures to specifically regulate Jmjd3 demethylase activity might be useful for manipulating macrophages to mount anti-helminth host defenses and tissue repair.

METHODS

Methods and any associated references are available in the online version of the paper at http://www.nature.com/natureimmunology/.

Accession codes. GEO: microarray data, GSE23180; ChIP-Seq data, GSE23297.

Note: Supplementary information is available on the Nature Immunology website.

ACKNOWLEDGMENTS

We thank all the colleagues in our laboratory, E. Kamada for secretarial assistance and Y. Fujiwara, M. Kumagai, R. Abe, N. Kitagaki and S. Yumikura for technical assistance. This work was supported by the Special Coordination Funds of the Japanese Ministry of Education, Culture, Sports, Science and Technology, and grants from the Ministry of Health, Labour and Welfare in Japan, the Global Center of Excellence Programs of Osaka University and Nagasaki University and the US National Institutes of Health (P01 AI070167). Computational time was provided by the Super Computer System at the Human Genome Center, Institute of Medical Science, The University of Tokyo. A.V. was partly supported by a Japanese government scholarship.

AUTHOR CONTRIBUTIONS

T. Satoh and O.T. designed and performed experiments. Y.K., T. Miyake, K.M., T.O. and T. Saitoh performed experiments. A.V., Y.T., D.M.S. and K. Nakai analyzed ChIP-Seq data. K. Yasuda and K. Nakanishi performed *N. brasiliensis* infection experiments. K.H., T. Matsuyama and K. Yui provided *Irf4*$^{-/-}$ mice. T.T. performed histological examination. O.T., T. Satoh and S.A. wrote the manuscript. S.A. supervised the project. A.V. and K.Y. contributed equally to this work.

COMPETING FINANCIAL INTERESTS

The authors declare no competing financial interest.

Published online at http://www.nature.com/natureimmunology/.
Reprints and permissions information is available online at http://npg.nature.com/reprintsandpermissions/.

1. Takeuchi, O. & Akira, S. Pattern recognition receptors and inflammation. *Cell* **140**, 805–820 (2010).
2. Medzhitov, R. Origin and physiological roles of inflammation. *Nature* **454**, 428–435 (2008).
3. Beutler, B. Microbe sensing, positive feedback loops, and the pathogenesis of inflammatory diseases. *Immunol. Rev.* **227**, 248–263 (2009).
4. Mantovani, A., Sozzani, S., Locati, M., Allavena, P. & Sica, A. Macrophage polarization: tumor-associated macrophages as a paradigm for polarized M2 mononuclear phagocytes. *Trends Immunol.* **23**, 549–555 (2002).
5. Gordon, S. Alternative activation of macrophages. *Nat. Rev. Immunol.* **3**, 23–35 (2003).
6. Benoit, M., Desnues, B. & Mege, J.L. Macrophage polarization in bacterial infections. *J. Immunol.* **181**, 3733–3739 (2008).
7. Bronte, V. & Zanovello, P. Regulation of immune responses by L-arginine metabolism. *Nat. Rev. Immunol.* **5**, 641–654 (2005).
8. Nair, M.G., Guild, K.J. & Artis, D. Novel effector molecules in type 2 inflammation: lessons drawn from helminth infection and allergy. *J. Immunol.* **177**, 1393–1399 (2006).
9. Nair, M.G. *et al.* Chitinase and Fizz family members are a generalized feature of nematode infection with selective upregulation of Ym1 and Fizz1 by antigen-presenting cells. *Infect. Immun.* **73**, 385–394 (2005).
10. Stein, M., Keshav, S., Harris, N. & Gordon, S. Interleukin 4 potently enhances murine macrophage mannose receptor activity: a marker of alternative immunologic macrophage activation. *J. Exp. Med.* **176**, 287–292 (1992).
11. Mantovani, A. *et al.* The chemokine system in diverse forms of macrophage activation and polarization. *Trends Immunol.* **25**, 677–686 (2004).
12. Verreck, F.A. *et al.* Human IL-23-producing type 1 macrophages promote but IL-10-producing type 2 macrophages subvert immunity to (myco)bacteria. *Proc. Natl. Acad. Sci. USA* **101**, 4560–4565 (2004).
13. Martinez, F.O., Gordon, S., Locati, M. & Mantovani, A. Transcriptional profiling of the human monocyte-to-macrophage differentiation and polarization: new molecules and patterns of gene expression. *J. Immunol.* **177**, 7303–7311 (2006).
14. Fleetwood, A.J., Lawrence, T., Hamilton, J.A. & Cook, A.D. Granulocyte-macrophage colony-stimulating factor (CSF) and macrophage CSF-dependent macrophage phenotypes display differences in cytokine profiles and transcription factor activities: implications for CSF blockade in inflammation. *J. Immunol.* **178**, 5245–5252 (2007).
15. Fleetwood, A.J., Dinh, H., Cook, A.D., Hertzog, P.J. & Hamilton, J.A. GM-CSF- and M-CSF-dependent macrophage phenotypes display differential dependence on type I interferon signaling. *J. Leukoc. Biol.* **86**, 411–421 (2009).
16. Medzhitov, R. & Horng, T. Transcriptional control of the inflammatory response. *Nat. Rev. Immunol.* **9**, 692–703 (2009).
17. Yamamoto, M. *et al.* Regulation of Toll/IL-1-receptor-mediated gene expression by the inducible nuclear protein IκBζ. *Nature* **430**, 218–222 (2004).
18. Kayama, H. *et al.* Class-specific regulation of pro-inflammatory genes by MyD88 pathways and IκBζ. *J. Biol. Chem.* **283**, 12468–12477 (2008).
19. Gilchrist, M. *et al.* Systems biology approaches identify ATF3 as a negative regulator of Toll-like receptor 4. *Nature* **441**, 173–178 (2006).
20. Charo, I.F. Macrophage polarization and insulin resistance: PPARγ in control. *Cell Metab.* **6**, 96–98 (2007).
21. Wei, G. *et al.* Global mapping of H3K4me3 and H3K27me3 reveals specificity and plasticity in lineage fate determination of differentiating CD4+ T cells. *Immunity* **30**, 155–167 (2009).
22. Barski, A. *et al.* High-resolution profiling of histone methylations in the human genome. *Cell* **129**, 823–837 (2007).
23. Schuettengruber, B., Chourrout, D., Vervoort, M., Leblanc, B. & Cavalli, G. Genome regulation by polycomb and trithorax proteins. *Cell* **128**, 735–745 (2007).
24. Hong, S. *et al.* Identification of JmjC domain-containing UTX and JMJD3 as histone H3 lysine 27 demethylases. *Proc. Natl. Acad. Sci. USA* **104**, 18439–18444 (2007).
25. Lan, F. *et al.* A histone H3 lysine 27 demethylase regulates animal posterior development. *Nature* **449**, 689–694 (2007).
26. De Santa, F. *et al.* The histone H3 lysine-27 demethylase Jmjd3 links inflammation to inhibition of polycomb-mediated gene silencing. *Cell* **130**, 1083–1094 (2007).
27. Matsushita, K. *et al.* Zc3h12a is an RNase essential for controlling immune responses by regulating mRNA decay. *Nature* **458**, 1185–1190 (2009).
28. De Santa, F. *et al.* Jmjd3 contributes to the control of gene expression in LPS-activated macrophages. *EMBO J.* **28**, 3341–3352 (2009).
29. Barradas, M. *et al.* Histone demethylase JMJD3 contributes to epigenetic control of INK4a/ARF by oncogenic RAS. *Genes Dev.* **23**, 1177–1182 (2009).
30. Agger, K. *et al.* The H3K27me3 demethylase JMJD3 contributes to the activation of the INK4A-ARF locus in response to oncogene- and stress-induced senescence. *Genes Dev.* **23**, 1171–1176 (2009).
31. Bowman, S.M. & Free, S.J. The structure and synthesis of the fungal cell wall. *Bioessays* **28**, 799–808 (2006).
32. Reese, T.A. *et al.* Chitin induces accumulation in tissue of innate immune cells associated with allergy. *Nature* **447**, 92–96 (2007).
33. Kreider, T., Anthony, R.M., Urban, J.F. Jr. & Gause, W.C. Alternatively activated macrophages in helminth infections. *Curr. Opin. Immunol.* **19**, 448–453 (2007).
34. Ishii, M. *et al.* Epigenetic regulation of the alternatively activated macrophage phenotype. *Blood* **114**, 3244–3254 (2009).
35. Da Silva, C.A., Hartl, D., Liu, W., Lee, C.G. & Elias, J.A. TLR-2 and IL-17A in chitin-induced macrophage activation and acute inflammation. *J. Immunol.* **181**, 4279–4286 (2008).
36. Mantovani, A. & Sica, A. Macrophages, innate immunity and cancer: balance, tolerance, and diversity. *Curr. Opin. Immunol.* **22**, 231–237 (2010).
37. Ahyi, A.N., Chang, H.C., Dent, A.L., Nutt, S.L. & Kaplan, M.H. IFN regulatory factor 4 regulates the expression of a subset of T_H2 cytokines. *J. Immunol.* **183**, 1598–1606 (2009).
38. Klein, U. *et al.* Transcription factor IRF4 controls plasma cell differentiation and class-switch recombination. *Nat. Immunol.* **7**, 773–782 (2006).
39. Zheng, Y. *et al.* Regulatory T-cell suppressor program co-opts transcription factor IRF4 to control T_H2 responses. *Nature* **458**, 351–356 (2009).
40. Honma, K. *et al.* Interferon regulatory factor 4 differentially regulates the production of T_H2 cytokines in naive vs. effector/memory CD4+ T cells. *Proc. Natl. Acad. Sci. USA* **105**, 15890–15895 (2008).
41. Honma, K. *et al.* Interferon regulatory factor 4 negatively regulates the production of proinflammatory cytokines by macrophages in response to LPS. *Proc. Natl. Acad. Sci. USA* **102**, 16001–16006 (2005).
42. Negishi, H. *et al.* Negative regulation of Toll-like-receptor signaling by IRF-4. *Proc. Natl. Acad. Sci. USA* **102**, 15989–15994 (2005).

ONLINE METHODS

Generation of *Jmjd3*$^{-/-}$ mice. The *Jmjd3* gene was isolated from genomic DNA extracted from embryonic stem cells (GSI-I) by PCR. The targeting vector was constructed by replacing a 4-kb fragment encoding the *Jmjd3* open reading frame (exons 14–21, including exons encoding the JmjC domain) with a neomycin-resistance gene cassette (*neo*), and herpes simplex virus thymidine kinase was inserted into the genomic fragment for negative selection. After the targeting vector was transfected into embryonic stem cells, G418 and gancyclovir doubly-resistant colonies were selected and screened by PCR; recombination was further confirmed by Southern blotting. These homologous-recombinant clones were microinjected into blastocysts derived from C57BL/6 mice and were transferred to pseudopregnant females. Matings of chimeric male mice to C57BL/6 female mice resulted in transmission of the mutant allele to the germline. Resulting *Jmjd3*$^{+/-}$ mice were intercrossed to generate *Jmjd3*$^{-/-}$ mice. All animal experiments were done with the approval of the Animal Research Committee of the Research Institute for Microbial Diseases, Osaka University.

Mice, cells and reagents. *Irf4*$^{-/-}$ mice were prepared as described[41]. Bone marrow–derived macrophages were generated in RPMI-1640 medium containing 10% (vol/vol) FCS, 50 μM 2-mercaptoethanol and 10 ng/ml GM-CSF (PeproTech) or 10 ng/ml M-CSF (PeproTech). Pam_3CSK_4 and R-848 were prepared as described[27]. LPS (*Salmonella minnesota* Re595) was from Sigma.

Generation of bone marrow–chimeric mice. Fetal liver cells were prepared from wild-type and *Jmjd3*$^{-/-}$ embryos (embryonic day 15.5). The cell suspensions were intravenously injected into lethally irradiated CD45.1 C57BL/6 mice. The chimeric mice were given neomycin and ampicillin in their drinking water for 4 weeks. The mice were analyzed at least 8 weeks after reconstitution. More than 90% of splenocytes from chimeric mice were CD45.2 positive.

Quantitative PCR analysis. Total RNA was isolated with TRIzol (Invitrogen), and reverse transcription was performed with ReverTra Ace (Toyobo) according to the manufacturer's instructions. For quantitative PCR, cDNA fragments were amplified by Realtime PCR Master Mix (Toyobo); fluorescence from the TaqMan probe for each cytokine was detected by a 7500 real-time PCR system (Applied Biosystems). To determine the relative induction of cytokine mRNA in response to various stimuli, the mRNA expression level of each gene was normalized to the expression level of 18S rRNA. The experiments were repeated at least twice.

Immunoblot analysis. M-BMMs were cultured for 4 h in medium without M-CSF (PeproTech) and then were collected and replated. M-BMMs were stimulated with M-CSF for times indicated in **Figure 5e** and were lysed with lysis buffer (20 mM Tris-HCl, pH 7.5, 150 mM NaCl, 1 mM EDTA and 1% (vol/vol) Nonidet P-40) containing complete mini protease inhibitor cocktail (Roche). Cell lysates were separated by standard SDS-PAGE and analyzed by immunoblot. Antibodies to the following proteins were used: phosphorylated Erk (Cell Signaling no. 9101), phosphorylated Akt (Cell Signaling 9271), phosphorylated p38 (Cell Signaling 9211), Akt (Cell Signaling 9272), p38 (Santa Cruz C-20), Erk (Santa Cruz K-23) and β-actin (Santa Cruz C-11).

Flow cytometry. Antibodies for flow cytometry were purchased from BD Biosciences and eBioscience. Cells were washed in ice-cold flow-cytometry buffer (2% (vol/vol) FCS and 2 mM EDTA in PBS, pH 7.5), then incubated with each antibody for 15 min and washed twice with flow-cytometry buffer. Intracellular cytokines were stained with Cytofix/Cytoperm Plus Fixation/Permeabilization Kit (BD Biosciences) according to the manufacturer's instructions. Data were acquired on a FACSCalibur flow cytometer (BD Biosciences) and analyzed with FlowJo (Tree Star).

Construction of *Jmjd3* expression plasmids. *Jmjd3* cDNA (corresponding to amino acid residues 1141–1641) was obtained by PCR from a mouse cDNA library, and a point mutation resulting in the A1388H substitution in the JmjC domain was introduced by site-directed mutagenesis (Stratagene). The full or mutated *Jmjd3* cDNAs were cloned into the pMRX-ires-puro vector for retrovirus production[43].

Retroviral transduction. Bone marrow cells were isolated from *Jmjd3*$^{-/-}$ mice that had been injected intraperitoneally 4 d earlier with 5 mg of 5-fluorouracil (Nacalai Tesque). Cells were cultured in stem cell medium (RPMI supplemented with 15% (vol/vol) FCS, 10 mM sodium pyruvate, 2 μM L-glutamine, 50 μM β-mercaptoethanol, 100 U/ml penicillin, 100 g/ml streptomycin, 100 ng/ml stem cell factor, 10 ng/ml IL-6 and 10 ng/ml IL-3). Then, 48 h later, these cells were transduced with retroviral supernatant (supplemented with stem cell factor, IL-6, IL-3 and 10 ng/ml of polybrene) on two successive days. Virus was produced by PlatE packaging cells transfected with various plasmids. After the second transduction, cells were washed and resuspended in macrophage growth medium (RPMI-1640 medium supplemented with 10% (vol/vol) FCS, 50 μM β-mercaptoethanol, 100 U/ml penicillin, 100 μg/ml streptomycin and 20 ng/ml M-CSF). After 3.5 d in culture, cells were washed once and macrophage growth medium with 2.5 μg/ml puromycin (InvivoGen) was added. The cells were cultivated for 2 d after changing of the medium and then were analyzed.

Chitin administration. Chitin (Sigma) was washed three times in PBS and then sonicated with a UR-20P device (Tomy) for 30 min on ice. After filtration with 100 μM cell strainer, chitin was diluted in 50 ml PBS. About 800 ng chitin was intraperitoneally injected, and PECs were collected 2 d after administration.

Responses to *N. brasiliensis* infection. Wild-type and *Jmjd3*$^{-/-}$ fetal liver–chimeric mice were subcutaneously inoculated with 300 third-stage larvae of *N. brasiliensis* 8 weeks after fetal liver transfer. On day 5 after infection, *N. brasiliensis*–inoculated mice were killed and perfused with PBS, and total RNAs from lungs were extracted. RNA was subjected to quantitative PCR for the analysis of expression of various genes. Nine days after infection, hilar lymph nodes were harvested, a single-cell suspension was prepared and cell numbers were counted. The lymph node cells were stimulated with anti-CD3 and anti-CD28. They were stained with CD4 and treated with cytofix (BD Biosciences), then stained with anti–IL-4 and anti–IFN-γ. Next, the cells were examined by flow cytometry. BAL was performed at 5 and 13 d after *N. brasiliensis* infection, and macrophages and eosinophils were enumerated on cytospin smears stained with Diff-Quick (Baxter Healthcare).

Microarray and chromatin immunoprecipitation–sequencing analysis. Microarray and ChIP-Seq protocols and data analysis are described in **Supplementary Methods**.

Statistics. Statistical significance was calculated with the two-tailed Student's *t*-test.

43. Saitoh, T. *et al.* TWEAK induces NF-κB2 p100 processing and long lasting NF-κB activation. *J. Biol. Chem.* **278**, 36005–36012 (2003).

Cell Host & Microbe
Article

Protein Kinase R Contributes to Immunity against Specific Viruses by Regulating Interferon mRNA Integrity

Oliver Schulz,[1] Andreas Pichlmair,[1,6] Jan Rehwinkel,[1] Neil C. Rogers,[1] Donalyn Scheuner,[2] Hiroki Kato,[5] Osamu Takeuchi,[5] Shizuo Akira,[5] Randal J. Kaufman,[2,3,4] and Caetano Reis e Sousa[1,*]
[1]Immunobiology Laboratory, Cancer Research UK, London Research Institute, London WC2A 3PX, UK
[2]Department of Biological Chemistry
[3]Department of Internal Medicine
[4]Howard Hughes Medical Institute
University of Michigan Medical School, Ann Arbor, MI 48109-0650, USA
[5]Department of Host Defense, Research Institute for Microbial Diseases, Osaka University, 3-1 Yamada-oka, Osaka 565-0871, Japan
[6]Present address: Director's Group, CeMM-Research Center for Molecular Medicine of the Austrian Academy of Sciences, Lazarettgasse 19/3, A-1090 Vienna, Austria
*Correspondence: caetano@cancer.org.uk
DOI 10.1016/j.chom.2010.04.007

SUMMARY

Cytosolic viral RNA recognition by the helicases RIG-I and MDA5 is considered the major pathway for IFN-α/β induction in response to RNA viruses. However, other cytoplasmic RNA sensors, including the double-stranded RNA-binding protein kinase R (PKR), have been implicated in IFN-α/β production, although their relative contribution and mechanism have been unclear. Using cells expressing nonfunctional PKR or reduced levels of kinase, we show that PKR is required for production of IFN-α/β proteins in response to a subset of RNA viruses including encephalomyocarditis, Theiler's murine encephalomyelitis, and Semliki Forest virus, but not influenza or Sendai virus. Surprisingly, although IFN-α/β mRNA induction is largely normal in PKR-deficient cells, much of that mRNA lacks the poly(A) tail, indicating that its integrity is compromised. Our results suggest that PKR plays a nonredundant role in IFN-α/β production in response to some but not all viruses, in part by regulating IFN-α/β mRNA stability.

INTRODUCTION

Immunity to viral infection is characterized by the production of antiviral cytokines, in particular type I interferons (IFN-α/β), which induce innate antiviral resistance and contribute to adaptive immunity (Le Bon and Tough, 2002; Samuel, 2001; Stark et al., 1998). IFN-α/β is primarily induced following the recognition of viral nucleic acids by host pattern recognition receptors (PRRs) that survey the extra- and intracellular milieu for the presence of viral genomes or viral replication intermediates (Pichlmair and Reis e Sousa, 2007; Takeuchi and Akira, 2008). For instance, several members of the toll-like receptor (TLR) family, including TLR3, TLR7, and TLR9, access the endosomal compartment, where they are triggered by viral double-stranded (ds) RNA, single-stranded RNA, and DNA, respectively, entering the cell from the extracellular milieu (Pichlmair and Reis e Sousa, 2007; Uematsu and Akira, 2007). In addition, all cells can respond to the presence of viral nucleic acids that have accessed the cytoplasm. The cytosolic PRRs involved in this process have not been fully identified, but recently the RNA helicases retinoic acid inducible gene I (RIG-I) and melanoma differentiation-associated factor-5 (MDA5) were shown to be essential for recognition of RNA viruses (Gitlin et al., 2006; Kato et al., 2005; Kato et al., 2006; Yoneyama et al., 2004). After binding to agonistic RNAs, both RIG-I and MDA5 interact with the adaptor IPS-1/MAVS/VISA/Cardif and initiate a signaling cascade that leads to activation of the transcription factors IRF-3 and IRF-7, which control transcription of the IFN-α and IFN-β genes (Pichlmair and Reis e Sousa, 2007; Takeuchi and Akira, 2008). Although both RIG-I and MDA5 can mediate responses to the synthetic dsRNA analog poly(I:C) in vitro, analysis of mice deficient for MDA5 has shown that this helicase is critical for responses to picornaviruses such as encephalomyocarditis virus (EMCV) and Theiler's murine encephalomyelitis virus (TMEV), whereas RIG-I mediates responses to other RNA viruses including Newcastle disease virus (NDV), vesicular stomatitis virus (VSV), Sendai virus (SeV), and influenza virus (Gitlin et al., 2006; Kato et al., 2005, 2006). This has led to the hypothesis that MDA5 and RIG-I have different specificities and discriminate between virus-specific forms of viral RNA. Consistent with that notion, we and others have recently shown that RIG-I but not MDA-5 triggering can ensue from recognition of 5′ triphosphate groups present in the genomes of many RNA viruses (Habjan et al., 2008; Hornung et al., 2006; Pichlmair et al., 2006; Rehwinkel et al., 2010). RNA agonists for MDA-5 have not been fully characterized but are thought to correspond to long molecules of dsRNA.

dsRNA can be found in the genome of some viruses but can also be generated during the process of viral replication. Interestingly, immunodetectable dsRNA (i.e., dsRNA >30 bp) is seen primarily in cells infected with DNA or positive-strand RNA viruses (Pichlmair et al., 2006; Weber et al., 2006), many

of which are recognized by MDA5. Such dsRNA also binds to and activates PKR, an enzyme that confers antiviral resistance but differs structurally and functionally from the RNA helicases (Williams, 1999, 2001). PKR belongs to the family of kinases that regulate cellular functions in response to stress and viral infection (Holcik and Sonenberg, 2005). The main function of PKR is to limit viral replication through phosphorylation of the α subunit of the translation initiation factor eIF-2, which results in shutdown of cellular and viral protein synthesis (Williams, 1999, 2001). Long before the discovery of MDA5 and RIG-I, PKR was proposed to act as a virus PRR involved in type I IFN induction. Some studies, including our own, found that PKR-deficient cells can be defective in IFN-α/β production in response to poly(I:C) (Diebold et al., 2003; McAllister and Samuel, 2009; Smith et al., 2001; Yang et al., 1995). However, PKR deficiency did not prevent IFN-α/β responses to NDV and, in some cases, IFN-α/β production could be restored in *PKR*$^{-/-}$ cells by pretreatment with type I IFN (Yang et al., 1995). The subsequent discovery of RIG-I and MDA5 led to the conclusion that PKR is largely unimportant for IFN-α/β induction (Pichlmair and Reis e Sousa, 2007; Takeuchi and Akira, 2008). However, some recent studies support a nonredundant role for the kinase in IFN-α/β responses to viral infection (Barry et al., 2009; Carpentier et al., 2007; Gilfoy and Mason, 2007) and raise the possibility that some but not all viruses induce IFN-α/β in a PKR-dependent manner.

Here we report that PKR is required for IFN-α/β production in response to a specific subset of RNA viruses including EMCV, TMEV, and Semliki Forest virus (SFV). Surprisingly, unlike RIG-I and MDA5, PKR does not act by inducing IFN-α/β gene transcription but rather by indirectly maintaining the integrity of newly synthesized IFN-α/β mRNA, thereby permitting its translation. Our data reveal a key and nonredundant role for PKR in sustaining the IFN response to some RNA viruses and help reconcile apparently conflicting observations in the literature on the role of PKR in type I IFN induction.

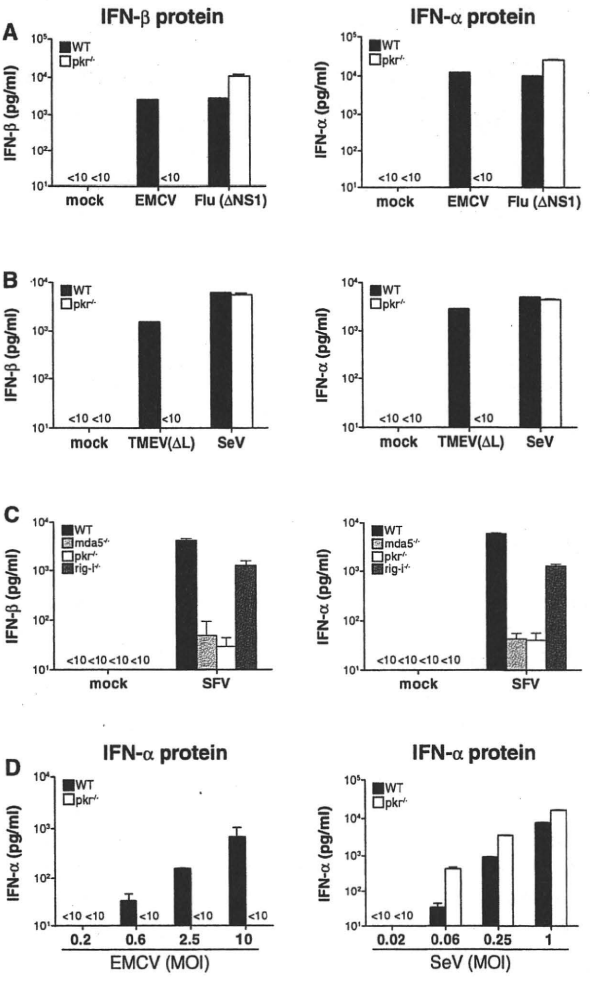

Figure 1. PKR Is Required for IFN-α/β Production by BM-DCs in Response to EMCV, TMEV, and SFV

BM-DCs (5 × 10^5/well) were infected with RNA viruses as indicated, and IFN-α/β accumulation in the culture supernatants was measured by ELISA after overnight culture. Data are the mean ± SD of triplicate wells.

(A) Production of IFN-β protein (left panel) and IFN-α protein (right panel) by BM-DCs infected with EMCV (moi = 10) or influenza virus (Flu [ΔNS1]) (moi = 1). Data are representative of at least three (influenza virus) and ten (EMCV) independent experiments.

(B) Production of IFN-β protein (left panel) and IFN-α protein (right panel) by BM-DCs infected with TMEV(ΔL) (moi = 10) or SeV (moi = 1). Data are representative of at least three (TMEV) and ten (SeV) independent experiments.

(C) IFN-α/β production in response to SFV is mainly dependent on MDA5. BM-DCs lacking either MDA5, RIG-I, or PKR were infected with SFV (moi = 10). Data shown are one out of two experiments with similar results.

(D) IFN-α production in relation to infectious dose for EMCV (left panel) and SeV (right panel). Data represent one of two experiments with similar results.

RESULTS

PKR Requirement for IFN-α/β Production Is Virus Specific

We re-examined the role of PKR in IFN production by infecting wild-type or PKR-deficient mouse bone marrow-derived dendritic cells (BM-DCs) in vitro with a panel of RNA viruses that are sensed primarily by MDA5, including EMCV, TMEV, or viruses that are recognized by RIG-I such as influenza virus and SeV. Production of IFN-α/β by PKR-deficient BM-DC was normal in response to wild-type or ΔNS1 influenza virus (influenza mutant lacking the interferon inhibitor NS1; Figure 1A and data not shown) or SeV (Figure 1B), as measured by IFN-α and IFN-β protein accumulation in culture supernatants. In contrast, EMCV and TMEV(ΔL), a TMEV mutant lacking the interferon antagonistic leader (L) protein, failed to induce measurable levels of IFN-α or IFN-β protein in the absence of PKR (Figures 1A and 1B). Like EMCV and TMEV, alphaviruses such as SFV generate considerable amounts of dsRNA in infected cells (see Figure S1A available online). IFN-α/β production in response to SFV was barely detectable in the absence of MDA5 and was reduced by 4-fold in *RIG-I*$^{-/-}$ BM-DCs (Figure 1C), indicating that SFV is recognized by MDA5 with a modest contribution from RIG-I (see also Figure 4). Importantly, IFN-α and IFN-β production after infection with SFV was also reduced by more than 100-fold in BM-DC lacking PKR (Figure 1C). IFN-α/β induction by EMCV but not SeV was PKR dependent at all doses tested

(Figure 1D), indicating that the virus-specific PKR dependence was not merely a quantitative effect.

We measured dsRNA content as well as cell viability after viral infection. The percentage of cells expressing dsRNA following infection with EMCV or SFV was higher for PKR-deficient than for wild-type BM-DC (Figure S1A), in line with the established role of PKR in suppressing viral replication (Williams, 1999, 2001). We found a slight increase in the percentage of dead cells in cultures of BM-DC lacking PKR (Figure S1B), although this effect was too small to account for the lack of IFN-α/β secretion by these cells. Thus, lack of virus replication or cell death cannot explain the impaired IFN-α/β responses in PKR-deficient DCs infected with picornaviruses or SFV.

To confirm these observations in another cell type, we analyzed IFN-α/β expression in MEFs. To circumvent virus-induced cytotoxicity in those cells, which was much more pronounced than in DCs (data not shown), MEFs were pre-treated with IFN-α/β. We used IFN A/D, a human IFN hybrid that does not cross-react with the ELISA antibodies used for measuring mouse IFN-α/β but acts like other IFNs to promote an antiviral state that protects the cells from cytopathic effects of viral infection (Rehberg et al., 1982). Like DCs, $PKR^{-/-}$ MEFs treated with IFN A/D mounted a normal IFN-α/β response after SeV infection but showed a severe defect in the response to EMCV (Figure 2A). We also used siRNA-mediated gene silencing to rule out that the effect was due to a secondary phenotype of the PKR-deficient cells. When infected with EMCV, MEFs treated with PKR-specific siRNA showed a 3-fold reduction in PKR levels (data not shown) and a 60% reduction in the level of IFN-α and IFN-β compared to MEFs treated with a control siRNA (Figure 2B). Consistent with the results in PKR-deficient cells, the PKR-specific siRNA did not impair the response to SeV (Figure 2B). Altogether, these observations suggest that PKR is required for IFN-α/β production in response to some RNA viruses and that the PKR dependence of the IFN-α/β response to any given virus correlates with reliance on the MDA5 pathway.

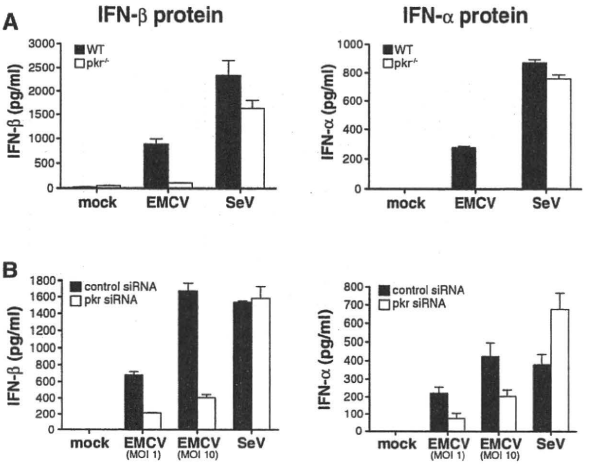

Figure 2. PKR Mediates IFN-α/β Production by MEFs in Response to EMCV

Immortalized MEFs (5×10^5/well) were stimulated with IFN A/D (1000 U/ml) for 2 hr prior to infection with EMCV or SeV. IFN-α/β accumulation in the culture supernatants was measured by ELISA after overnight culture. Data are the mean ± SD of triplicate wells.

(A) IFN-β protein (left panel) and IFN-α protein (right panel) from $PKR^{-/-}$ and wild-type MEFs infected with EMCV (moi = 10) or SeV (moi = 1).

(B) IFN-β protein (left panel) and IFN-α protein (right panel) from siRNA-treated MEFs after infection with EMCV or SeV (moi = 1). Data are representative of four independent experiments.

Phosphorylation of eIF-2α Is Not Necessary for IFN-α/β Production in Response to PKR-Dependent Viruses

Most biological effects of PKR are mediated through phosphorylation of eIF-2α (Holcik and Sonenberg, 2005; Williams, 1999, 2001). To test whether eIF-2α phosphorylation is required for the PKR-dependent production of IFN-α/β in response to EMCV and SFV, we used cells with a homozygous Ser-to-Ala mutation at the eIF-2α phosphorylation site (Ser51) (Scheuner et al., 2001). In contrast to wild-type cells, eIF-2α mutant MEFs (eIF2A/A) did not phosphorylate eIF-2α in response to poly(I:C) (Figure 3A). Nevertheless, eIF2A/A MEFs showed no defect in their ability to produce IFN-α or IFN-β proteins in response to stimulation with poly(I:C) (data not shown) or upon infection with EMCV or SFV (Figure 3B). We conclude that phosphorylation of eIF-2α is not required for PKR-dependent IFN-α/β production.

PKR Regulates IFN-β mRNA Integrity Rather Than Transcriptional Activation in Cells Infected with EMCV

We next asked whether PKR is necessary for EMCV- or SFV-dependent transcriptional induction of the IFN-α/β genes. Because the IFN-α ELISA detects multiple IFN-α subtypes, we focused on IFN-β, which is encoded by a single gene, allowing us to directly correlate the protein and transcript levels. The latter were determined by quantitative PCR of cDNA generated by random hexamer oligonucleotide priming of RNA extracted from infected cells. As expected (Kato et al., 2005, 2006), SeV infection induced the appearance of IFN-β mRNA in a RIG-I-dependent, MDA-5-independent manner, which correlated with IFN-β protein expression (Figures 4A and 4B). Consistent with the role of MDA5 as a PRR for SFV and EMCV, $MDA5^{-/-}$ cells failed to accumulate IFN-β mRNA or produce IFN-β protein in response to either virus (Figures 4A and 4B). In contrast, to our surprise, IFN-β mRNA was induced >1000-fold in PKR-deficient cells infected with EMCV (Figure 4B) even though IFN-β protein was not detectable (Figure 4A). Similarly, infection with SFV led to upregulation of IFN-β mRNA in $PKR^{-/-}$ DCs at levels 100-fold and 10-fold higher than in DCs lacking either MDA5 or RIG-I, respectively (Figure 4B), but did not result in IFN-β protein production (Figure 4A). Taken together, our data suggest that, although MDA5 and PKR are both essential for driving IFN-α/β production in response to EMCV and SFV, the mechanism of their action is different. Unlike MDA5, PKR is largely dispensable for the induction of IFN-α/β mRNA but appears to act posttranscriptionally to regulate protein production.

It was intriguing that $PKR^{-/-}$ cells produced little IFN-β protein despite seemingly normal induction of IFN-β mRNA following infection with EMCV. To gain further insight into this issue, we analyzed IFN-β mRNA from EMCV-infected cells by northern blot. This analysis indicated that IFN-β mRNA levels were in fact 6- to 8-fold lower in $PKR^{-/-}$ BM-DC compared to $PKR^{+/+}$

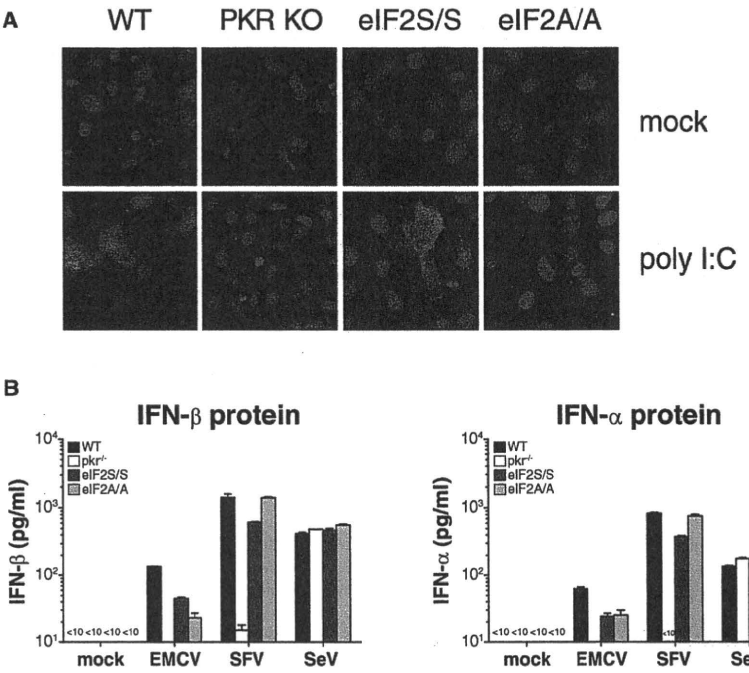

Figure 3. Phosphorylation of eIF-2α Is Not Necessary for IFN-α/β Production in Response to PKR-Dependent Viruses

(A) Confocal analysis of eIF-2α phosphorylation in Ser51 mutant MEFs (eIF2A/A) and control MEFs. Cells were stimulated with poly(I:C) for 6 hr and stained with mAbs specific for phospho-eIF-2α and dsRNA (K1), as well as the nuclear dye DRAQ5. Phospho-eIF-2α and dsRNA staining are shown in green and red, respectively.

(B) IFN-β protein (left panel) and IFN-α protein (right panel) from eIF-2A/A and control eIF-2S/S MEFs infected with EMCV (moi = 10), SFV (moi = 10), or SeV (moi = 1). Data shown are from one out of three experiments, and represent mean ± SD.

cells (Figures 5A and 5B). It was conceivable that the lower IFN-β mRNA levels in PKR-deficient cells arose from a failure to up-regulate MDA5, which is itself IFN inducible (Kang et al., 2002). Consistent with this notion, $PKR^{-/-}$ cells showed decreased levels of MDA5 mRNA upon infection with EMCV but not SeV, which could be corrected by pretreatment with IFN-A/D (Figure S2). Notably, IFN A/D pretreatment also restored IFN-β mRNA levels in EMCV-infected PKR-deficient DC to within 1- to 3-fold of the levels in wild-type cells (Figure 5B). However, IFN A/D pretreatment failed to rescue IFN-β protein production by DC (Figure 5C), as noted for MEFs (see above).

Unexpectedly, northern blot analysis of RNA from cells infected with EMCV revealed the presence of two bands for IFN-β with different apparent molecular sizes (Figures 5A and 5B). The lower molecular size band was especially prominent in PKR-deficient cells: it accounted for 10%–20% of the total IFN-β mRNA in $PKR^{+/+}$ DC but up to 60% in $PKR^{-/-}$ DC (Figures 5A, 5B, and 5D). The shorter form of IFN-β mRNA was not seen upon infection with SeV and was not especially prominent in response to transfection with poly(I:C) (Figures 5A, 5B, and 5D). The size difference between the short and long forms was a few hundred bases, which could correspond to the poly(A) tract of the mRNA. Consistent with that notion, the shorter form had an apparent molecular size of around 750 bases (Figures 5A and 5B), similar to that reported for the IFN-β cDNA lacking the poly(A) tail (Higashi et al., 1983). To test the possibility that the lower molecular size band corresponded to IFN-β mRNA lacking a poly(A) tail, we hybridized dT oligonucleotides to RNA from infected cells and digested with RNase H. After enzymatic removal of the poly(A) tail, all IFN-β mRNA showed an electrophoretic mobility similar to that of the lower band seen in RNA from $PKR^{-/-}$ cells not treated with RNase H (Figure 5D). Importantly, the mRNA from EMCV-infected $PKR^{-/-}$ cells did not show a further shift in electrophoretic mobility, indicating that it was already deadenylated (Figure 5D). Furthermore, when dT oligonucleotides were used instead of random hexamer oligonucleotides to generate complementary DNA, quantitative PCR revealed a profound difference in the levels of IFN-β mRNA between $PKR^{+/+}$ and $PKR^{-/-}$ cells (Figure 5E). This effect was EMCV specific, because we found no difference between hexamer and oligo dT-primed IFN-β cDNA in cells infected with SeV (Figure 5E), consistent with the northern blot analysis (Figures 5B and 5D). We also compared hexamer and oligo dT-primed cDNA for several other inducible or constitutively expressed genes, including GAPDH, IL-6, TNF-α, and RPS-16, and observed that the ratio of cDNA between wild-type and $PKR^{-/-}$ cells following infection with EMCV or SeV remained unchanged (Figure S3). These results indicate that the lack of a poly(A) tail in EMCV-infected cells is specific to IFN-β mRNA and not reflective of a generic deadenylation of all cellular mRNAs. We conclude that, in the absence of PKR, most of the IFN-β mRNA generated in response to EMCV infection lacks the poly(A) tail. This could impair its translation and explain the absence of IFN-β protein synthesis by EMCV-infected $PKR^{-/-}$ cells.

Serum Levels of IFN-β Are Reduced in PKR-Deficient Mice after Infection with EMCV

To extend these observations to an in vivo setting, we infected wild-type and PKR-deficient mice with EMCV and measured IFN-β in the serum at 20 hr postinfection. Serum IFN-β levels in wild-type mice were generally low regardless of genetic background (Figures 6A–6C), and mRNA for IFN-β in tissues was below the detection limit, precluding analysis of its adenylation status (data not shown). Nevertheless, we consistently observed even lower levels of serum IFN-β protein in mice lacking PKR (Figures 6A–6C). This was true in experiments when wild-type 129/Sv mice were compared to $PKR^{-/-}$ mouse on a mixed 129 Sv/C57BL/6 background (Figure 6A) but also when $PKR^{-/-}$ mice that had been backcrossed more than ten times to the

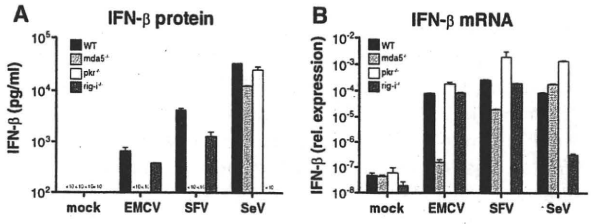

Figure 4. PKR Deficiency Disproportionately Reduces IFN-β Protein versus mRNA

BM-DCs (5 × 10^5/well) were infected with RNA viruses for 12 hr as indicated. IFN-β protein in the culture supernatants and IFN-β mRNA in total cDNA from lysed cells (synthesized using random hexamer primers) were measured by ELISA and quantitative PCR, respectively. Data are the mean ± SD of triplicate wells. (A) Production of IFN-β protein and (B) IFN-β mRNA from DCs lacking MDA5, RIG-I, or PKR following infection with EMCV (moi = 10), SFV (moi = 10), or SeV (moi = 1). Data are representative of two independent experiments with similar results.

C57BL/6 strain were compared to wild-type mice of that strain (Figure 6B). Finally, PKR deficiency led to a reduction in serum IFN-β levels in *MyD88*$^{-/-}$ mice infected with EMCV (Figure 6C), excluding the possibility that the effect of PKR was downstream of the TLR7 pathway, which can contribute to IFN responses to ssRNA viruses in vivo. In conclusion, our results and those of others (Barry et al., 2009) confirm a role for PKR in generating an optimal IFN response to EMCV and SFV in vivo.

DISCUSSION

The notion that PKR is involved in the induction of IFN-α/β has largely been dismissed by the discovery of the RNA helicases RIG-I and MDA5 and associated signaling pathways (Pichlmair and Reis e Sousa, 2007; Takeuchi and Akira, 2008). RNA viruses are increasingly classified by their ability to stimulate RIG-I, MDA5 or a combination of both (Gitlin et al., 2006; Kato et al., 2005;, 2006). Here, we compared viruses representing different ends of this spectrum for their ability to induce IFN-α/β in the absence or presence of PKR. In agreement with previous studies using NDV (Smith et al., 2001; Yang et al., 1995), PKR was not required for IFN-α/β production in cells infected with RIG-I-dependent viruses such as influenza and SeV. In contrast, IFN-α/β production in response to the picornaviruses EMCV and TMEV, both capable of triggering MDA5, was greatly reduced in cells lacking PKR. Furthermore, SFV, which we find to be primarily recognized via MDA5, also required PKR for IFN protein production, as reported recently (Barry et al., 2009). Two previous reports have also implicated PKR in cytokine production after infection with TMEV and West Nile virus (Carpentier et al., 2007; Gilfoy and Mason, 2007), two viruses that are recognized, at least in part, via MDA5 (Fredericksen et al., 2008). Thus, it is intriguing to speculate that PKR may promote IFN-α/β production to MDA5- but not to RIG-I-dependent viruses. Interestingly, a requirement for PKR in IFN-α/β responses to the putative MDA5 agonist, poly(I:C), had been noted in some studies (Diebold et al., 2003; McAllister and Samuel, 2009; Smith et al., 2001; Yang et al., 1995). We find that such PKR dependence is variable, perhaps because many preparations of poly(I:C) additionally stimulate RIG-I and TLR3 pathways, and is therefore best observed using viruses that show a strong dependence on MDA5 for IFN-α/β induction (O.S., A.P., and C.R.S., unpublished data). The correlation between MDA5 and PKR dependence of antiviral IFN-α/β responses may arise from the fact that PKR and MDA5 can be activated by long dsRNA (Lemaire et al., 2008), which is not produced to any great extent by

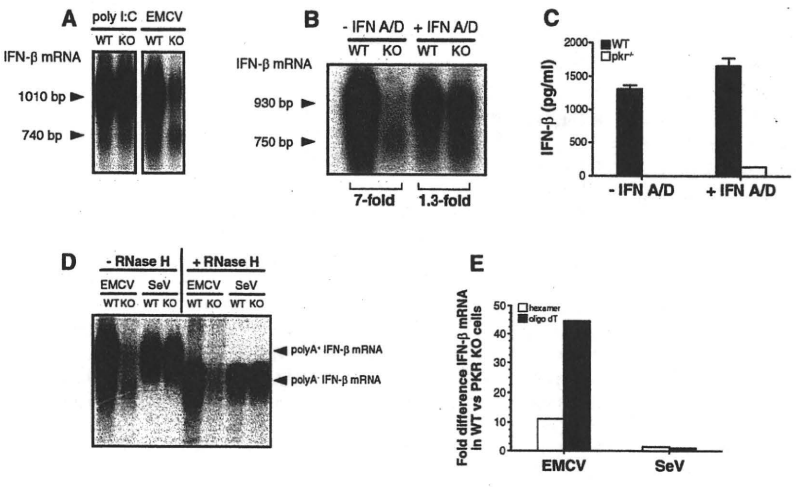

Figure 5. Deadenylated IFN-β mRNA in EMCV-Infected *PKR*$^{-/-}$ Cells

(A–C) BM-DCs (5 × 10^5/well) were transfected with poly(I:C) (10 μg/well) for 6 hr or infected with EMCV (moi = 10) for 9 hr in the absence or presence of IFN A/D (1000 U/ml) as indicated. (A and B) IFN-β mRNA was analyzed by northern blot, and the position of two distinct species of IFN-β mRNA is indicated by arrowheads. The size of the different mRNA species was calculated by comparing their electrophoretic mobility to a molecular size marker in the form of a ssRNA ladder. Numbers below picture represent fold difference between samples from *PKR*$^{+/+}$ and *PKR*$^{-/-}$ cells as determined by phosphoimager analysis. (C) IFN-β protein in the supernatant from the same cultures as in (B) was measured by ELISA. Data are the mean ± SD of triplicate wells and are representative of three independent experiments with similar results.

(D) Detection of polyA$^+$ and polyA$^-$ forms of IFN-β mRNA by northern blot. Total RNA was isolated from BM-DCs infected with EMCV (moi = 10) or SeV (moi = 1) for 12 and 6 hr, respectively. Where indicated, RNA samples were treated with oligo-dT ± RNase H. Arrowheads indicate position of polyA$^+$ and polyA$^-$ IFN-β mRNA.

(E) RNA from cells treated as in (D) was analyzed by quantitative PCR using random hexamer (open bars) or oligo dT oligonucleotides (filled bars) to generate cDNA. Relative expression of IFN-β mRNA in *PKR*$^{+/+}$ versus *PKR*$^{-/-}$ cells was calculated by analyzing the Ct values for each amplification curve and converting them into fold difference using the formula $2^{(-\Delta Ct)}$.

Data in (D) and (E) are representative of two experiments.

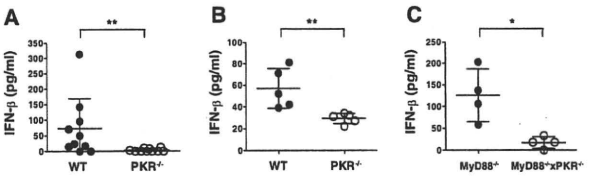

Figure 6. PKR Promotes IFN-β Protein Production in Response to Infection with EMCV In Vivo

IFN-β protein was measured in the serum of mice that had been infected with EMCV 20 hr earlier.

(A) Wild-type (129 Sv) and $PKR^{-/-}$ mice (mixed 129 Sv/C57BL/6 background), $p < 0.006$ ($n = 10$).

(B) Wild-type (C57BL/6) and $PKR^{-/-}$ mice (C57BL/6 background), $p < 0.008$ ($n = 5$).

(C) $MyD88^{-/-}$ and $MyD88^{-/-} \times PKR^{-/-}$ mice, $p < 0.03$ ($n = 4$).

(A–C) Dots represent individual mice, bars are mean ± SD. Data in each panel are representative of two independent experiments with similar results. Paired data were analyzed using a two-tailed Mann-Whitney test.

many of the RIG-I-dependent viruses (Pichlmair et al., 2006; Weber et al., 2006). However, it should be noted that PKR can also be activated upon infection with RIG-I-dependent viruses, possibly through 5′-triphosphate RNA containing short stem loops (Nallagatla et al., 2007). Therefore, one would need to envisage that different RNA agonists elicit different PKR responses and that PKR has a hitherto unappreciated role in controlling IFN-α/β production when it has been activated by infection with viruses that generate specific forms of dsRNA.

EMCV has emerged as the prototypic MDA5-dependent virus (Gitlin et al., 2006; Kato et al., 2006), and a previous study showed a reduction in IFN-α/β expression following EMCV infection of cells expressing a dominant-negative form of PKR (Der and Lau, 1995). This is consistent with our findings, although, in contrast to that earlier report, we could find no evidence that PKR contributes significantly to the induction of IFN-α/β genes. Although PKR can promote the activation of nuclear factor kappa B (Kumar et al., 1994), its ability to activate IRF-3 and -7, the critical transcription factors in induction of IFN-α/β genes (Honda and Taniguchi, 2006; Sato et al., 2000), has not been formally demonstrated. Our data are consistent with the current concept that signaling via RIG-I-like helicases, but not through PKR, leads to transcription of the IFN-α and IFN-β genes (Yoneyama et al., 2005). Nevertheless, our results support a role for PKR in regulating the quality of IFN-α/β mRNA in the context of viral infection. How PKR regulates this process or what are the molecular targets downstream of PKR is currently not understood. We have been able to rule out a role for the translation initiation factor eIF-2α, the best-characterized PKR substrate, by showing that phosphorylation of eIF-2α is not required for IFN production in response to EMCV infection. Given that eIF-2α phosphorylation is crucial for the virus-induced translation stop (Garcia et al., 2006) and apoptosis (Kaufman, 1999; Scheuner et al., 2006), these results indicate that PKR promotes IFN-α/β protein expression by a different mechanism.

This mechanism appears to involve regulation of IFN-α/β mRNA integrity, as we found that much of the IFN-β mRNA from $PKR^{-/-}$ cells after infection with EMCV appears truncated. Any role for PKR in preventing this process is not only specific to infection with some viruses but also mRNA specific, as we did not observe loss of integrity in other mRNAs, be they from inducible or constitutively expressed genes. Further analysis of IFN-β mRNA from EMCV-infected cells suggests that the truncated form of IFN-β mRNA might correspond to mRNA that has lost its poly(A) tail. The expression of many cytokines is controlled by posttranscriptional mechanisms that regulate various aspects of RNA biology, especially mRNA stability and decay (Anderson, 2008). Indeed, IFN-β mRNA contains several destabilizing elements, including a class II AU-rich element that promotes asynchronous deadenylation and leads to the accumulation of poly(A)-negative intermediates (Paste et al., 2003). The molecules that bind to the destabilizing elements in IFN-β mRNA or that regulate the degradation of the poly(A) tail remain poorly characterized (Anderson, 2008; Raj and Pitha, 1993) and, therefore, leave open many possibilities as to how PKR regulates IFN-β mRNA integrity in the context of EMCV infection. For example, PKR impacts on eIF4E phosphorylation via the B56α regulatory subunit of protein phosphatase 2A, thereby potentially affecting translation and deadenylation of mRNA in a manner independent of eIF2α (Xu and Williams, 2000). Alternatively, PKR may act by antagonizing virus-specific factors that promote destabilization of IFN-β mRNA rather than having a direct role in regulating IFN-α/β mRNAs. Although we do not understand the mechanism at present, our data nevertheless provide a possible explanation as to why IFN-β mRNA, despite being present in $PKR^{-/-}$ cells, is not expressed at the protein level.

In sum, our data support a role for PKR in regulating the expression of IFN-α/β proteins and demonstrate that PKR is required coordinately with a member of the RIG-I-like helicase family, MDA5, to induce an IFN response to certain RNA viruses. Our study further reveals that PKR may act primarily in establishing and/or maintaining the polyadenylation status of IFN-α/β mRNA, adding to our understanding of IFN-α/β induction after virus infection and revealing a hitherto unappreciated role for mRNA stability in the process.

EXPERIMENTAL PROCEDURES

Reagents

IFN A/D was a gift from I. Kerr (Cancer Research UK). Poly(I:C) was from Amersham Biosciences. Recombinant murine GM-CSF was made at Cancer Research UK. SiRNA specific for mouse PKR (Prkr-3) and human PRMT (protein arginine methyltransferase; control siRNA) were from QIAGEN. The target sequences for murine PKR and human PRMT are CAGCTCGTCTATGA CAAGTAA and AAAGATTACTACTTTGACTCC, respectively. Anti-dsRNA antibody (clone K1) was from English & Scientific Consulting Bt. Polyclonal anti-phospho-eIF-2α (Ser51) was from New England Biolabs.

The plasmid pGEM-IFN-β was generated by PCR amplification of full-length IFN-β from BM-DCs stimulated with SeV and subsequent cloning of the PCR product into pGEM-T vector (Promega). The sequences for murine IFN-β forward and reverse primers were 5′-ATGAACAACAGGTGGATCC and 5′-GG CATCAACTGACAGGTCTT, respectively.

The plasmid pBABE-puro-LargeT was a gift from G. Peters (Cancer Research UK).

Animals and Cells

Strain 129 SvEv mice were obtained from Taconic. $PKR^{-/-}$ mice (Yang et al., 1995) on a mixed 129 SvEv x C57Bl6 background were originally obtained from H. Unger (University of Veterinary Medicine, Vienna, Austria) and were maintained in the animal facility of CRUK (Clare Hall, South Mimms, UK) under

specific pathogen-free conditions. For in vivo experiments, mice were fully backcrossed (ten generations) to C57BL/6 or to mice deficient in MyD88. BM-DCs were generated in RPMI 1640 medium containing 10% FCS, 2 mM glutamine, 50 μM 2-mercaptoethanol, 100 units/ml penicillin, 100 μg/ml streptomycin, and GM-CSF (~10-ng/ml). Wild-type (129-SvEv Tac) and *PKR*$^{-/-}$ MEFs were prepared from 12.5 day embryos by standard protocols. MEFs were used as primary cells or after immortalization with retrovirus expressing large T antigen prepared from supernatants of Phoenix cells transfected with pBABE-puro-LargeT. Immortalized MEFs were selected on puromycin (final concentration 2 μg/ml) for 2 weeks and were grown in DMEM medium containing 10% FCS, 2 mM glutamine, 100 units/ml penicillin, and 100 μg/ml streptomycin. Primary MEFs were grown in DMEM containing 10% filtered, non-heat-inactivated FCS, 1 × MEM amino acids, 1 × non-essential amino acids, 50 μM 2-mercaptoethanol, 100 units/ml penicillin, and 100 μg/ml streptomycin.

Viruses and Cytokine Induction Assays

Influenza A/PR/8/34 and ΔNS1 were a gift from T. Muster (Vienna). SFV and EMCV were a gift from I. Kerr. TMEV(ΔL) was a gift from T. Michiels (Brussels). SeV was obtained from LGC Promochem/ATCC.

BM-DCs or MEFs were seeded in 24 plates at 5 × 10^5 cells per ml and cultured with different viruses for 12–15 hr unless indicated otherwise. This time point was chosen because for some viruses (i.e., EMCV), IFN-α/β protein became detectable only at around 10 hr after infection (data not shown). IFN A/D (1000 U/ml) was added to MEF cultures 2 hr prior to infection. Mice were infected intravenously with EMCV (10^6 pfu/mouse). Supernatants or mouse sera were assayed for cytokine content by sandwich ELISA. IFN-α (multiple subtypes) was measured by ELISA as described previously (Diebold et al., 2003), and IFN-β was measured using an ELISA Kit (R&D Systems).

Flow Cytometry

BM-DCs were seeded in 24 plates at 5 × 10^5 cells per ml and infected with EMCV or SFV overnight. Cells were fixed in 4% paraformaldehyde, permeabilized using 0.1% saponin, and stained with anti-CD11c mAb (Becton Dickinson) and anti-dsRNA mAb followed by appropriate secondary antibodies. For assessment of cell viability, BM-DCs were fixed and stained with LIVE/DEAD fixable dead cell dye (Invitrogen) as recommended by the manufacturer. Samples were run on a FACS Calibur (Becton Dickinson), and data were analyzed using FlowJo software (Treestar).

Confocal Microscopy

MEFs were grown on coverslips overnight and stimulated for 6 hr with dsRNA by transfecting poly(I:C) (1 μg/well) complexed with Lipofectamine 2000 (Invitrogen). Cells were fixed in 4% paraformaldehyde, permeabilized in 0.1% Triton X-100, and stained with anti-dsRNA and anti-phospho-eIF-2α antibodies followed by secondary antibodies including Alexa 488-conjugated anti-rabbit, Alexa 546-conjugated anti-mouse, and DRAQ5 (Invitrogen). Coverslips were mounted on a slide and images taken with a laser-scanning confocal microscope (LSM 510; Zeiss).

PKR Knockdown

MEFs were seeded at 2.5 × 10^4 cells/well in 24-well plates in DMEM medium without antibiotics. Cells were transfected twice (at 0 and +24 hr) with PKR-specific siRNA or control siRNA (40 pmol/well) using the transfection reagent Lipofectamine 2000 (Invitrogen). At the end of 48 hr cells were either stimulated with IFN A/D (1000 U/ml) for 1–2 hr prior to infection with viruses as indicated or stimulated with IFN A/D (1000 U/ml) alone overnight for analysis of PKR protein by western blot.

PCR and Northern Blot

Total RNA was isolated from infected or uninfected cells using the RNeasy kit (QIAGEN) combined with a DNA digestion step (DNase set, QIAGEN). Single-stranded cDNA was synthesized using SuperScript II (Invitrogen) and random hexamer or poly dT primers. Quantitative PCR amplification was carried out using TaqMan universal master mix (Applied Biosystems) and predeveloped TaqMan assay reagents (containing primers and fluorescent probe) for murine IFN-β, MDA5, 18 s rRNA, IL-6, TNF-α, RPS-16, and GAPDH (Applied Biosystems) on an ABI 7900HT thermal cycler (Applied Biosystems).

For northern blotting, total RNA was separated by gel electrophoresis on an 1.5% agarose gel. RNA was transfered by capillary action to a nylon membrane (Hybond-N$^+$; Amersham Biosciences), crosslinked to the membrane with UV light, and hybridized with [a^{32}P]-dCTP and [a^{32}P]-dATP (Perkin Elmer) labeled probes. Antisense deoxyribo probes specific for murine IFN-β were generated by linear PCR amplification of a full-length template (generated through conventional PCR amplification of pGEM-IFN-β) using the reverse primer for IFN-β. For poly(A) tail digestion, total RNA was hybridized to dT(15) oligonucleotides and treated with RNase H (USB Europe GMBH) for 2 hr at 37°C.

SUPPLEMENTAL INFORMATION

Supplemental Information includes three figures and can be found with this article at doi:10.1016/j.chom.2010.04.007.

ACKNOWLEDGMENTS

This work was funded by Cancer Research UK and in part by National Institutes of Health (NIH) grants DK042394, HL052173, and HL057346 (to R.J.K.). C.R.S. acknowledges the financial support of the Fondation Bettencourt-Schueller. R.J.K. is an investigator of the Howard Hughes Medical Institute. J.R. is a recipient of FEBS and HFSP long-term fellowships. We thank Ian Kerr for EMCV and SFV, Thomas Muster for Flu(ΔNS1), Thomas Michiels for TMEV(ΔL), and Hermann Unger for *PKR*$^{-/-}$ mice. We are grateful to Sandra S. Diebold and members of the Immunobiology Lab for advice and critical review of the manuscript.

Received: June 2, 2009
Revised: February 16, 2010
Accepted: April 7, 2010
Published: May 19, 2010

REFERENCES

Anderson, P. (2008). Post-transcriptional control of cytokine production. Nat. Immunol. *9*, 353–359.

Barry, G., Breakwell, L., Fragkoudis, R., Attarzadeh-Yazdi, G., Rodriguez-Andres, J., Kohl, A., and Fazakerley, J.K. (2009). PKR acts early in infection to suppress Semliki Forest virus production and strongly enhances the type I interferon response. J. Gen. Virol. *90*, 1382–1391.

Carpentier, P.A., Williams, B.R., and Miller, S.D. (2007). Distinct roles of protein kinase R and toll-like receptor 3 in the activation of astrocytes by viral stimuli. Glia *55*, 239–252.

Der, S.D., and Lau, A.S. (1995). Involvement of the double-stranded-RNA-dependent kinase PKR in interferon expression and interferon-mediated antiviral activity. Proc. Natl. Acad. Sci. USA *92*, 8841–8845.

Diebold, S.S., Montoya, M., Unger, H., Alexopoulou, L., Roy, P., Haswell, L.E., Al-Shamkhani, A., Flavell, R., Borrow, P., and Reis e Sousa, C. (2003). Viral infection switches non-plasmacytoid dendritic cells into high interferon producers. Nature *424*, 324–328.

Fredericksen, B.L., Keller, B.C., Fornek, J., Katze, M.G., and Gale, M., Jr. (2008). Establishment and maintenance of the innate antiviral response to West Nile Virus involves both RIG-I and MDA5 signaling through IPS-1. J. Virol. *82*, 609–616.

Garcia, M.A., Gil, J., Ventoso, I., Guerra, S., Domingo, E., Rivas, C., and Esteban, M. (2006). Impact of protein kinase PKR in cell biology: from antiviral to antiproliferative action. Microbiol. Mol. Biol. Rev. *70*, 1032–1060.

Gilfoy, F.D., and Mason, P.W. (2007). West Nile virus-induced interferon production is mediated by the double-stranded RNA-dependent protein kinase PKR. J. Virol. *81*, 11148–11158.

Gitlin, L., Barchet, W., Gilfillan, S., Cella, M., Beutler, B., Flavell, R.A., Diamond, M.S., and Colonna, M. (2006). Essential role of mda-5 in type I IFN responses to polyriboinosinic:polyribocytidylic acid and encephalomyocarditis picornavirus. Proc. Natl. Acad. Sci. USA *103*, 8459–8464.

Habjan, M., Andersson, I., Klingström, J., Schümann, M., Martin, A., Zimmermann, P., Wagner, V., Pichlmair, A., Schneider, U., Mühlberger, E., et al. (2008). Processing of genome 5′ termini as a strategy of negative-strand RNA viruses to avoid RIG-I-dependent interferon induction. PLoS ONE *3*, e2032. 10.1371/journal.pone.0002032.

Higashi, Y., Sokawa, Y., Watanabe, Y., Kawade, Y., Ohno, S., Takaoka, C., and Taniguchi, T. (1983). Structure and expression of a cloned cDNA for mouse interferon-beta. J. Biol. Chem. *258*, 9522–9529.

Holcik, M., and Sonenberg, N. (2005). Translational control in stress and apoptosis. Nat. Rev. Mol. Cell Biol. *6*, 318–327.

Honda, K., and Taniguchi, T. (2006). IRFs: master regulators of signalling by Toll-like receptors and cytosolic pattern-recognition receptors. Nat. Rev. Immunol. *6*, 644–658.

Hornung, V., Ellegast, J., Kim, S., Brzozka, K., Jung, A., Kato, H., Poeck, H., Akira, S., Conzelmann, K.K., Schlee, M., et al. (2006). 5′-Triphosphate RNA is the ligand for RIG-I. Science *314*, 994–997.

Kang, D.C., Gopalkrishnan, R.V., Wu, Q., Jankowsky, E., Pyle, A.M., and Fisher, P.B. (2002). mda-5: an interferon-inducible putative RNA helicase with double-stranded RNA-dependent ATPase activity and melanoma growth-suppressive properties. Proc. Natl. Acad. Sci. USA *99*, 637–642.

Kato, H., Sato, S., Yoneyama, M., Yamamoto, M., Uematsu, S., Matsui, K., Tsujimura, T., Takeda, K., Fujita, T., Takeuchi, O., et al. (2005). Cell type-specific involvement of RIG-I in antiviral response. Immunity *23*, 19–28.

Kato, H., Takeuchi, O., Sato, S., Yoneyama, M., Yamamoto, M., Matsui, K., Uematsu, S., Jung, A., Kawai, T., Ishii, K.J., et al. (2006). Differential roles of MDA5 and RIG-I helicases in the recognition of RNA viruses. Nature *441*, 101–105.

Kaufman, R.J. (1999). Double-stranded RNA-activated protein kinase mediates virus-induced apoptosis: a new role for an old actor. Proc. Natl. Acad. Sci. USA *96*, 11693–11695.

Kumar, A., Haque, J., Lacoste, J., Hiscott, J., and Williams, B.R. (1994). Double-stranded RNA-dependent protein kinase activates transcription factor NF-kappa B by phosphorylating I kappa B. Proc. Natl. Acad. Sci. USA *91*, 6288–6292.

Le Bon, A., and Tough, D.F. (2002). Links between innate and adaptive immunity via type I interferon. Curr. Opin. Immunol. *14*, 432–436.

Lemaire, P.A., Anderson, E., Lary, J., and Cole, J.L. (2008). Mechanism of PKR Activation by dsRNA. J. Mol. Biol. *381*, 351–360.

McAllister, C.S., and Samuel, C.E. (2009). The RNA-activated protein kinase enhances the induction of interferon-beta and apoptosis mediated by cytoplasmic RNA sensors. J. Biol. Chem. *284*, 1644–1651.

Nallagatla, S.R., Hwang, J., Toroney, R., Zheng, X., Cameron, C.E., and Bevilacqua, P.C. (2007). 5′-triphosphate-dependent activation of PKR by RNAs with short stem-loops. Science *318*, 1455–1458.

Paste, M., Huez, G., and Kruys, V. (2003). Deadenylation of interferon-beta mRNA is mediated by both the AU-rich element in the 3′-untranslated region and an instability sequence in the coding region. Eur. J. Biochem. *270*, 1590–1597.

Pichlmair, A., and Reis e Sousa, C. (2007). Innate recognition of viruses. Immunity *27*, 370–383.

Pichlmair, A., Schulz, O., Tan, C.P., Naslund, T.I., Liljestrom, P., Weber, F., and Reis e Sousa, C. (2006). RIG-I-mediated antiviral responses to single-stranded RNA bearing 5′-phosphates. Science *314*, 997–1001.

Raj, N.B., and Pitha, P.M. (1993). 65-kDa protein binds to destabilizing sequences in the IFN-beta mRNA coding and 3′ UTR. FASEB J. *7*, 702–710.

Rehberg, E., Kelder, B., Hoal, E.G., and Pestka, S. (1982). Specific molecular activities of recombinant and hybrid leukocyte interferons. J. Biol. Chem. *257*, 11497–11502.

Rehwinkel, J., Tan, C.P., Goubau, D., Schulz, O., Pichlmair, A., Bier, K., Robb, N., Vreede, F., Barclay, W., Fodor, E., and Reis e Sousa, C. (2010). RIG-I detects viral genomic RNA during negative-strand RNA virus infection. Cell *140*, 397–408.

Samuel, C. (2001). Antiviral actions of interferons. Clin. Microbiol. Rev. *14*, 778–809.

Sato, M., Suemori, H., Hata, N., Asagiri, M., Ogasawara, K., Nakao, K., Nakaya, T., Katsuki, M., Noguchi, S., Tanaka, N., et al. (2000). Distinct and essential roles of transcription factors IRF-3 and IRF-7 in response to viruses for IFN-alpha/beta gene induction. Immunity *13*, 539–548.

Scheuner, D., Song, B., McEwen, E., Liu, C., Laybutt, R., Gillespie, P., Saunders, T., Bonner-Weir, S., and Kaufman, R.J. (2001). Translational control is required for the unfolded protein response and in vivo glucose homeostasis. Mol. Cell *7*, 1165–1176.

Scheuner, D., Patel, R., Wang, F., Lee, K., Kumar, K., Wu, J., Nilsson, A., Karin, M., and Kaufman, R.J. (2006). Double-stranded RNA-dependent protein kinase phosphorylation of the alpha-subunit of eukaryotic translation initiation factor 2 mediates apoptosis. J. Biol. Chem. *281*, 21458–21468.

Smith, E.J., Marie, I., Prakash, A., Garcia-Sastre, A., and Levy, D.E. (2001). IRF3 and IRF7 phosphorylation in virus-infected cells does not require double-stranded RNA-dependent protein kinase R or Ikappa B kinase but is blocked by Vaccinia virus E3L protein. J. Biol. Chem. *276*, 8951–8957.

Stark, G., Kerr, I., Williams, B., Silverman, R., and Schreiber, R. (1998). How cells respond to interferons. Annu. Rev. Biochem. *67*, 227–264.

Takeuchi, O., and Akira, S. (2008). MDA5/RIG-I and virus recognition. Curr. Opin. Immunol. *20*, 17–22.

Uematsu, S., and Akira, S. (2007). Toll-like receptors and type I interferons. J. Biol. Chem. *282*, 15319–15323.

Weber, F., Wagner, V., Rasmussen, S.B., Hartmann, R., and Paludan, S.R. (2006). Double-stranded RNA is produced by positive-strand RNA viruses and DNA viruses but not in detectable amounts by negative-strand RNA viruses. J. Virol. *80*, 5059–5064.

Williams, B.R. (1999). PKR; a sentinel kinase for cellular stress. Oncogene *18*, 6112–6120.

Williams, B.R. (2001). Signal integration via PKR. Sci. STKE *2001*, RE2.

Xu, Z., and Williams, B.R. (2000). The B56alpha regulatory subunit of protein phosphatase 2A is a target for regulation by double-stranded RNA-dependent protein kinase PKR. Mol. Cell. Biol. *20*, 5285–5299.

Yang, Y.L., Reis, L.F., Pavlovic, J., Aguzzi, A., Schafer, R., Kumar, A., Williams, B.R., Aguet, M., and Weissmann, C. (1995). Deficient signaling in mice devoid of double-stranded RNA-dependent protein kinase. EMBO J. *14*, 6095–6106.

Yoneyama, M., Kikuchi, M., Natsukawa, T., Shinobu, N., Imaizumi, T., Miyagishi, M., Taira, K., Akira, S., and Fujita, T. (2004). The RNA helicase RIG-I has an essential function in double-stranded RNA-induced innate antiviral responses. Nat. Immunol. *5*, 730–737.

Yoneyama, M., Kikuchi, M., Matsumoto, K., Imaizumi, T., Miyagishi, M., Taira, K., Foy, E., Loo, Y.M., Gale, M., Jr., Akira, S., et al. (2005). Shared and unique functions of the DExD/H-box helicases RIG-I, MDA5, and LGP2 in antiviral innate immunity. J. Immunol. *175*, 2851–2858.

OPEN ACCESS Freely available online PLoS PATHOGENS

Co-ordinated Role of TLR3, RIG-I and MDA5 in the Innate Response to Rhinovirus in Bronchial Epithelium

Louise Slater[1,2,3], Nathan W. Bartlett[1,2,3], Jennifer J. Haas[1,2,3], Jie Zhu[4], Simon D. Message[1,5], Ross P. Walton[1,2,3], Annemarie Sykes[1,2,3,5], Samer Dahdaleh[1], Deborah L. Clarke[3,6], Maria G. Belvisi[3,6], Onn M. Kon[3,5], Takashi Fujita[7], Peter K. Jeffery[4], Sebastian L. Johnston[1,2,3,5], Michael R. Edwards[1,2,3]*

1 Department of Respiratory Medicine, National Heart & Lung Institute, Imperial College London, London, United Kingdom, **2** MRC & Asthma UK Centre in Allergic Mechanisms of Asthma, London, United Kingdom, **3** Centre for Respiratory Infection, London, United Kingdom, **4** Lung Pathology, National Heart & Lung Institute, Imperial College London, London, United Kingdom, **5** Imperial Healthcare NHS Trust, London, United Kingdom, **6** Respiratory Pharmacology, National Heart & Lung Institute, Imperial College London, London, United Kingdom, **7** Institute of Virus Research, Kyoto University, Kyoto, Japan

Abstract

The relative roles of the endosomal TLR3/7/8 versus the intracellular RNA helicases RIG-I and MDA5 in viral infection is much debated. We investigated the roles of each pattern recognition receptor in rhinovirus infection using primary bronchial epithelial cells. TLR3 was constitutively expressed; however, RIG-I and MDA5 were inducible by 8–12 h following rhinovirus infection. Bronchial epithelial tissue from normal volunteers challenged with rhinovirus *in vivo* exhibited low levels of RIG-I and MDA5 that were increased at day 4 post infection. Inhibition of TLR3, RIG-I and MDA5 by siRNA reduced innate cytokine mRNA, and increased rhinovirus replication. Inhibition of TLR3 and TRIF using siRNA reduced rhinovirus induced RNA helicases. Furthermore, *IFNAR1* deficient mice exhibited RIG-I and MDA5 induction early during RV1B infection in an interferon independent manner. Hence anti-viral defense within bronchial epithelium requires co-ordinated recognition of rhinovirus infection, initially via TLR3/TRIF and later via inducible RNA helicases.

Citation: Slater L, Bartlett NW, Haas JJ, Zhu J, Message SD, et al. (2010) Co-ordinated Role of TLR3, RIG-I and MDA5 in the Innate Response to Rhinovirus in Bronchial Epithelium. PLoS Pathog 6(11): e1001178. doi:10.1371/journal.ppat.1001178

Editor: Raymond J. Pickles, University of North Carolina at Chapel Hill, United States of America

Received February 3, 2010; **Accepted** October 1, 2010; **Published** November 4, 2010

Funding: This work was supported by grants from the British Lung Foundation (BLF Grant P06/3) and Medical Research Council (MRC G0601236). MRE is supported by a Fellowship from Asthma UK (RF07/04). SDM was supported by a Medical Research Council Clinical Research Fellowship, and a British Medical Association H.C. Roscoe Fellowship. Further support was obtained through British Lung Foundation/Severin Wunderman Family Foundation Lung Research Program Grant P00/2, Asthma UK Grants 02/027 and 05/067, Wellcome Trust Grant 083567/Z/07/Z for the Centre for Respiratory Infection, Imperial College, and the National Institute for Health Research Biomedical Research Centre funding scheme. The funders had no role in study design, data collection and analysis, decision to publish, or preparation of the manuscript.

Competing Interests: The authors have declared that no competing interests exist.

* E-mail: michael.edwards@imperial.ac.uk

Introduction

Human rhinovirus (RV) belongs to the *Picornaviridae* family and are implicated in an extensive range of human respiratory disorders including the common cold, viral bronchiolitis, and exacerbations of asthma and chronic obstructive pulmonary disease [1–5]. RV are classified as major or minor group based on receptor usage, or RNA identity as RV-A and RV-B. RVs of both major and minor groups are associated with human disease. Recently, this phylogeny been changed to include the newly designated RV-C group which represent a distinct group of RV [6]. RV of all groups generally infect the epithelial cells of both the upper and lower airway, and are responsible for the induction of a range of mediators including pro-inflammatory cytokines and growth factors [7–11], type I interferon (IFN)-β and type III IFN-λs [12]. Pro-inflammatory cytokines contribute to the duration and severity of RV induced illnesses [13–16]. Recently, primary human bronchial epithelial cells (HBECs) from asthmatics were found to be defective in IFN-β and IFN-λ mRNA and protein, [17,18], providing a likely explanation for the increased vulnerability to virus induced asthma exacerbations and enhanced symptom severity observed [16,19]. Understanding the mechanisms responsible for these deficiencies in asthma, as well as identifying new anti-inflammatory therapies requires a detailed understanding of the innate reponses to RV infection.

Much is now known about the signal transduction pathways utlised by viruses to induce cytokines and IFNs. RNA viruses are initially sensed through pattern recognition receptors (PRRs), such as recognition of dsRNA by endosomal Toll-like receptor (TLR)-3, [20,21] or ssRNA by endosomal TLR7/8 [22,23]. TLR3 utilises the adaptor TIR domain-containing adapter inducing IFN-β (TRIF), to activate IκB kinase (IKK-ι/ε) and TANK binding kinase-1 (TBK-1), and IKK-β activating interferon regulatory factor (IRF)-3 and NF-κB, transcription factors required for IFN-β gene expression. Within the intracellular compartment, exists a second set of PRRs, the RNA helicases, including retinoic acid inducible gene (RIG-I) [24], melanoma differentiation associated gene-5 (MDA5) [25], and the inhibitory protein LGP2 [26,27]. The helicases signal via their caspase recruitment domains (CARD), to adaptor inducing interferon-β (CARDIF) [28], (also known as IPS-1, MAVS and VISA, [29–31]), and activate TBK1, IKK-ι/ε and IKK-β, and hence IRF3 and NF-κB. Both RIG-I and MDA5 have been implicated in IFN-α/β production in various model systems. MDA5 recognises high molecular weight dsRNA [32], while the specificity of RIG-I has been marked with controversy. While originally identified as a dsRNA binding

Author Summary

Host-pathogen interactions are mediated by pattern recognition receptors that identify conserved structures of micro-organisms that are distinct from self. During a viral infection, important pattern recognition receptors include the endosomal Toll-like receptors (TLRs), and a second set of cytoplasmic pattern recognition receptors known as the RNA helicases. Many studies have highlighted the importance of TLR3, TLR7/8 and the RNA helicases in providing robust anti-viral immunity via interferon induction and inflammation. Both endosomal TLR and cytoplasmic RNA helicase mediated pathways are believed to exist as separate yet non-redundant entities; however, little thought is given to why both systems exist, and few studies also consider how both pathways together contribute to anti-viral immunity. Using models of rhinovirus infection in primary bronchial epithelial cell culture *in vitro* and experimental infection in mouse and human models *in vivo*, we show that the RNA helicases are preferentially induced early in the infection cycle via TLR3 mediated signaling events, and work in a co-ordinated, systematic manner. The results help understand the complex events that determine effective innate immunity to rhinovirus infection and how these processes contribute to virus induced exacerbations of asthma and chronic obstructive pulmonary disease.

helicase [24], RIG-I has recently been shown to bind low molecular weight dsRNA [32] and also 5′-triphosphorylated ssRNA [33,34]. The 5′-triphosphorylated ssRNA binding preferences of RIG-I suggest it is unable to recognize Picornavirus infections [33,35]; which do not synthesis 5′-triphosphorylated RNA molecules. The relative importance of TLR3, MDA5 or RIG-I in viral infections has been partly defined by cells derived from *TLR3*$^{-/-}$ [21], *RIG-I*$^{-/-}$ or *MDA5*$^{-/-}$ mice [35,36], however the importance of each PRR, including their exclusive or redundant roles in various infection models, and their direct relevance to human disease remains a subject of much debate.

In order to understand the recognition of RV infection, and the induction of both pro-inflammatory cytokines and IFNs, we investigated the role of TLR3/7/8, RIG-I and MDA5 in the innate response to RV infection in primary HBECs, the target cell for RV infection within the lower airway *in vivo*. We found that HBECs did not respond to the ligand R-848. Importantly, TLR3, and RNA helicase mediated signaling was required for maximal IFN-β, IFN-λ and pro-inflammatory cytokine gene expression, showing that RIG-I is required for anti-viral defense against Picornaviruses. Furthermore, RIG-I and MDA5 were virus inducible genes, induced early via a TLR3/TRIF pathway, indicating that TLR3 acts as an initial endosomal sensor and must induce the RNA helicases for maximal anti-viral defense during the course of infection. Thus the innate response to RV infection requires co-ordinated endosomal, and cytoplasmic recognition pathways, both of which contribute to IFN and cytokine production.

Results

Primary HBECs express TLR3, and RNA helicases RIG-I and MDA5, which are RV inducible genes with similar expression kinetics to RV induced IFN-β and IFN-λ

We first sought to assess the relationship between TLR3/7/8, and the RNA helicases in RV infection in bronchial epithelial cells. Initial studies showed that HBECs encoded mRNA and protein for TLR3, but did not induce IFN-β, IFN-λ, RIG-I or MDA5 mRNA in response to the TLR7/8 ligand R848 (Table S1 in Supporting Information S1), consistent with other studies showing that lung bronchial epithelial, alveolar and airway smooth muscle cells do not respond to TLR7/8 agonists [9,37,38]. The presence and/or absence and virus induction of TLR3 and RNA helicases was then investigated. Time course analysis in HBECs demonstrated that IFN-β was induced by 8 h post infection, and 4 h for IFN-λs post RV1B infection. IFN-β peaked at 12 h and remained at high levels until 48 h, while the IFN-λs remained elevated from 12 h and peaked at 48 h (Figure 1A–C). In the same experiments, RIG-I and MDA5 mRNA levels were also measured, and were induced by RV1B by 8 h, peaked by 18 h post infection and remained at high level until 48 h post infection (Figure 1D–E). At the protein level, RIG-I and MDA5 protein were both observed by 8 h following RV1B infection, and showed maximal levels at 18–24 h (Figure 1F). Uninfected cells and cells sampled at time 0 h exhibited almost non-detectable expression of RIG-I and MDA5 protein, suggesting that in the absence of active infection, RIG-I and MDA5 proteins are absent or expressed at very low level. TLR3 protein however was present in both infected and uninfected cells, and the levels did not change over the time course of RV1B infection. Similar data was observed for TLR3 mRNA (data not shown). The cytoplasmic staining of RIG-I and MDA5 were confirmed using immunofluorescence, with RV1B and IFN-β inducing both RIG-I (Figure 1G *upper panel*) and MDA5 (Figure 1G *lower panel*) at 24 h post treatment in HBECs, compared to cells treated with medium, or RV1B infected cells stained with a secondary antibody only.

RIG-I and MDA5 are induced in columnar bronchial epithelial cells upon experimental RV challenge *in vivo*

In order assess the baseline expression and the RV mediated induction of RIG-I and MDA5 protein in bronchial epithelium *in vivo*, bronchial biopsies were taken from 15 normal adult volunteers before experimental RV16 infection (baseline) or at day 4 post infection and stained for RIG-I and MDA5 by immunohistochemistry. Representative staining of biopsy samples are presented in Figure 2A–E. The degree of epithelial staining for RIG-I and MDA5 protein were scored quantitatively, and presented in Figure 2F. RIG-I (A) and MDA5 (C) had little staining at baseline, and MDA5 was increased at day 4 post RV16 infection, (Figure 2D). Scoring of columnar epithelial staining (F) showed that MDA5 at day 4 was significantly higher than baseline ($p<0.05$), however RIG-I levels were not significantly different at day 4 versus baseline (Figure 2B).

TLR3, RIG-I and MDA5 are required for maximal RV induced IFN-β, and IFN-λ

The PRRs involved in RV infection and induction of innate responses are largely unknown. In order to assess the role of TLR3, RIG-I and MDA5 in RV induced IFNs we used RNA interference with specific small interfering RNA (siRNA) to knockdown each PRR in HBECs *in vitro*, prior to RV infection. Initial experiments demonstrated that siRNA generated >75% knockdown of target mRNA at 24 h post treatment, and this knockdown was evident until 48 h post treatment (data not shown). Therefore, siRNA was delivered 24 h before infection, and total RNA harvested 24 h post RV1B infection, giving a total siRNA transfection time of 48 h. The knockdown of each target mRNA was confirmed in each experiment, and knockdown of target protein also confirmed at 48 h post transfection (Figure 3A–H). Also, experiments were performed

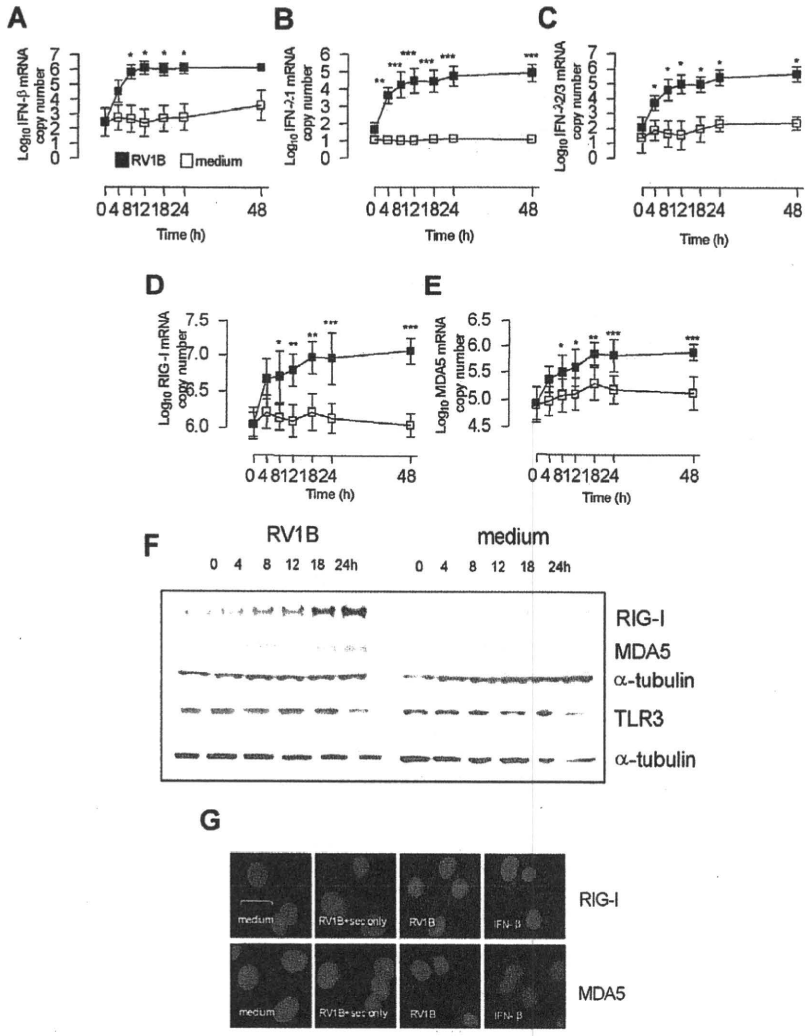

Figure 1. Kinetics of RV1B induced IFN-β, IFN-λs, RIG-I and MDA5 mRNA and protein expression in HBECs. HBECs were infected with RV1B or treated with medium and RNA and protein analysed over time. RV1B induced IFN-β (A), IFN-λ1 (B) and IFN-λ2/3 mRNA (C) in a time dependent manner, visible by 4 h, and peaking at 12–48 h. RV1B infection also induced RIG-I (D) and MDA5 mRNA (E), in a time dependent manner, peaking at 18–48 h. RV1B infection also induced RIG-I and MDA5 protein (F) in a similar time dependent manner, visible by 8 h post infection by western blotting. Medium treated cells exhibited little or no RIG-I or MDA5 protein during the timecourse. TLR3 protein levels were present in medium treated cells, and did not change during the course of RV1B infection. Immunofluorescence identified both cytoplasmic RIG-I and MDA5 to be induced after RV1B or IFN-β treatment at 24 h, compared to medium treated cells, or cells stained with secondary antibody only. Horizontal line indicates 20 μm scale. Staining for both helicases was observed within the cytoplasm (in green, G). *$p<0.05$, **$p<0.01$, ***$p<0.001$, RV1B infected versus medium treated cells. mRNA data was generated from 6 independent experiments utilizing 3 independent HBEC donors, 2 experiments per donor.

doi:10.1371/journal.ppat.1001178.g001

in the absence of RV infection to examine the effects of siRNA on endogenous IFN and pro-inflammatory cytokine gene expression. Each siRNA did not significantly induce any of the IFNs or pro-inflammatory cytokines studied (Table S2 & S3 in Supporting Information S1). Furthermore, RIG-I and MDA5 siRNA were highly specific, RIG-I siRNA did not affect endogenous MDA5 gene expression, and MDA5 siRNA did not affect endogenous RIG-I gene expression (data not shown). TLR3, RIG-I and MDA5 siRNA all reduced RV1B induced IFN-β compared to control siRNA (Figure 4A,D,G respectively). In contrast, siRNA targeting RIG-I did not reduce IFN-λ1 mRNA, (Figure 4E) however siRNA specific for TLR3 and MDA5 reduced IFN-λ1 (Figure 4B,H respectively). RIG-I siRNA enhanced RV induced IFN-λ2/3 mRNA (Figure 4F), while both MDA5 and TLR3 reduced RV1B induced IFN-λ2/3 (Figure 4C,I). These data suggest that TLR3, RIG-I and MDA5 are all required for IFN-β, and TLR3 and MDA5 for IFN-λ, however the importance of RIG-I in IFN-λs is less clear. To confirm these findings, we next used siRNA specific for the TLR3 adaptor TRIF, and the RNA helicase adaptor Cardif. We found that RV1B induced IFN-β and IFN-λ1 mRNA expression was inhibited by both siRNA to TRIF and Cardif, while IFN-λ2/3 was inhibited by TRIF siRNA only compared to control siRNA (Figure S1).